

STATICS AND DYNAMICS OF SUPER ELLIPTICAL
HOMOGENEOUS AND FGM PLATES

by

Seyit Çeribaşı

B.S., Civil Engineering, Boğaziçi University, 1998

M.S., Civil Engineering, Boğaziçi University, 2000

Submitted to the Institute for Graduate Studies in
Science and Engineering in partial fulfilment of
the requirements for the degree of
Doctor of Philosophy

Graduate Program in Civil Engineering

Boğaziçi University

2007

ACKNOWLEDGEMENTS

I would like to express my sincere thanks to my thesis supervisor, Prof. Dr. Gülay Altay for her invaluable guidance, continuous support, and helpful suggestions. She has always been supportive for the preparation of this thesis.

My sincere gratitude is also due to the members of my advisory committee Prof. Dr. Dr. M. Cengiz Dökmeci, Prof. Dr. Turan Özturan, Prof. Dr. Muhittin Söylemez and Prof. Dr. Semih S. Tezcan, for their useful suggestions and comments.

Heartfelt thanks to Pınar Günçan, Işıl Sanrı and H. Bora Keskin for their precious encouragement and assistance during preparation of my thesis.

ABSTRACT

STATICS AND DYNAMICS OF SUPER ELLIPTICAL HOMOGENEOUS AND FGM PLATES

In this study super elliptical plates are statically and dynamically analyzed. This class of plates includes a wide range of shapes varying from an ellipse to a rectangle. Although studies on the extreme boundaries of the super elliptical shapes (circle, ellipse, and rectangle) are extensive, contributions on the mid shapes are very limited. The studies are mostly concentrated on dynamics, thermal, and buckling behavior of the plates but not on static behavior. Kirchhoff plate model with isotropic and homogeneous material is studied. The first part of this study is concentrated on static behavior of the super elliptical plates under uniformly distributed surface load. For static analyses clamped boundary is assumed. The partial differential plate equations are solved by Galerkin method. The study is conducted for 10 super elliptical shapes and 14 central plate dimension ratios. The second part of the study deals with the dynamic behavior of super elliptical plates. Free vibration of simply supported plates is investigated and Ritz method is employed for the solution of the governing plate equations. The effect of Poisson's ratio, which can not be neglected for round edged simply supported plates, is examined in detail. The results of the study are presented in graphical and tabular forms and compared with previously obtained results of the available literature. In the last part of the study, functionally graded material (FGM) Kirchhoff plates have been investigated. For static analysis of the FGM plates, uniformly distributed surface load and clamped boundary is assumed and Galerkin method is employed. In addition to this, free vibration characteristics of simply supported FGM plates are studied by using Ritz method. The Poisson's ratios of the plates are assumed to be constant, but their Young's moduli vary in the thickness direction functionally. The objective of this part is to investigate the influence of volume fractions and the component materials on static and dynamic behavior of this class of plates.

ÖZET

HOMOJEN VE FGM SÜPER ELİPTİK PLAKLARIN STATİK VE DİNAMİĞİ

Bu çalışmada süper eliptik plaklar statik ve dinamik olarak analiz edilmiştir. Bu tür plaklar bir elipsten dikdörtgene kadar değişen birçok şekli kapsar. Her ne kadar süper eliptik plakların sınır şekilleri (daire, elips ve dikdörtgen) üzerine kapsamlı çalışmalar yapılmışsa da, ara şekilleri üzerine yapılan katkılar çok sınırlıdır. Çalışmalar plakların statik davranışları ihmal edilerek çoğunlukla dinamik, termal ve burkulma davranışı üzerine yoğunlaşmıştır. Burada izotropik, homojen malzemeli Kirchhoff plak modeli üzerine çalışılmıştır. Bu çalışmanın ilk kısmı süper eliptik plakların düzgün yayılı yüzey yükleri altındaki statik davranışına yoğunlaşmıştır. Statik analizde sabit mesnetli çevre koşulları kabul edilmiştir. Kısmi diferansiyel plak denklemleri Galerkin metoduyla çözülmüştür. Çalışma 10 süper eliptik şekil ve 14 plak boyut oranı için yürütülmüştür. Çalışmanın ikinci kısmı süper eliptik plakların dinamik davranışı ile ilgilidir. Basit mesnetli plakların serbest titreşimleri araştırılmış ve plak denklemlerinin çözümünde Ritz metodu kullanılmıştır. Yuvarlak kenarlı, basit mesnetli plaklarda ihmal edilemeyen Poisson oranının etkisi detaylı olarak incelenmiştir. Çalışmanın sonuçları grafik ve tablo şeklinde sunulmuş olup mevcut referansların sonuçlarıyla karşılaştırılmıştır. Çalışmanın son kısmında malzemesi bir fonksiyona bağlı olarak değişen (FGM) Kirchhoff plakları incelenmiştir. FGM plakların statik analizi için düzgün yayılı yüzey yükü ve sabit mesnetli çevre koşulu kabulleri yapılmıştır ve Galerkin metodu kullanılmıştır. Buna ek olarak FGM plakların serbest titreşim özellikleri Ritz metodu kullanılarak çalışılmıştır. Plakların Poisson oranları sabit kabul edilmiş, fakat elastisite modüllerinin kalınlık yönünde bir fonksiyona bağlı olarak değiştiği kabul edilmiştir. Bu bölümün amacı hacim oranlarının ve malzeme bileşenlerinin bu tür plakların statik ve dinamik davranışları üzerine olan etkisini incelemektir.

TABLE OF CONTENTS

ACKNOWLEDGEMENTS.....	iii
ABSTRACT.....	iv
ÖZET	v
LIST OF FIGURES	viii
LIST OF TABLES.....	x
LIST OF SYMBOLS	xiii
1. INTRODUCTION	1
1.1. Homogeneous Plates.....	1
1.2. Functionally Graded Material (FGM) Plates	3
1.3. Summary of the Numerical Analyses	5
2. PLATE MODEL	6
3. STATIC ANALYSES OF SUPER ELLIPTICAL CLAMPED PLATES BY MESHLESS GALERKIN METHOD	9
3.1. Basic Assumptions and Equations.....	9
3.2. Solution by Galerkin’s Method.....	11
3.3. Integration over the Super Elliptical Region	13
3.4. Presentation of the Results.....	15
3.5. Comparison of Results.....	21
3.6. Relation between Internal Forces and Displacements	21
3.7. Effect of Rounded Corners on Bending Moment Values	24
4. FREE VIBRATION OF SIMPLY SUPPORTED SUPER ELLIPTICAL PLATES BY RITZ METHOD	26
4.1. Basic Assumptions and Equations.....	26

4.2. Solution by Ritz Method.....	29
4.3. Presentation of the Results of Dynamic Analyses.....	33
5. STATIC ANALYSES OF FUNCTIONALLY GRADED SUPER ELLIPTICAL PLATES.....	45
5.1. Material Properties.....	45
5.2. Basic Equations and Assumptions.....	48
5.3. Results of Static Analyses.....	50
6. FREE VIBRATION OF SIMPLY SUPPORTED FGM SUPER ELLIPTICAL PLATES.....	53
6.1. Basic Equations and Assumptions.....	53
6.2. Results of the Free Vibration Analyses.....	55
7. CONCLUSIONS AND RECOMMENDATIONS.....	59
APPENDIX: : FREE VIBRATION EXAMPLE PREPARED BY USING MATHEMATICA 5.2.....	61
REFERENCES.....	73

LIST OF FIGURES

Figure 2.1.	Undeformed and deformed geometries of an edge of a plate in various Plate theories.....	8
Figure 3.1.	Super elliptical plates having the boundary equation $(x^{2n}/a^{2n}) + (y^{2n}/a^{2n})=1$	10
Figure 3.2.	Change of the deflection parameter $w_{max}(D/q_0)$ of clamped super elliptical plate obtained by the trial function of $r=2$ with respect to a/b ratio	16
Figure 3.3.	Change of the deflection parameter $w_{max}(D/q_0)$ of clamped super elliptical plate obtained by the trial function of $r=4$ with respect to a/b ratio	17
Figure 3.4.	Change of the deflection parameter $w_{max}(D/q_0)$ of clamped super elliptical plate obtained by the trial function of $r=6$ with respect to a/b ratio.....	18
Figure 3.5.	Change of the deflection parameter $w_{max}(D/q_0)$ of clamped super elliptical plate obtained by the trial function of $r=8$ with respect to a/b ratio.....	19
Figure 3.6.	Convergence of the deflection parameter $w_{max}(D/q_0)$ of clamped super elliptical plate of $a/b=1$ with respect to	19
Figure 3.7.	Convergence of the deflection parameter $w_{max}(D/q_0)$ of clamped super elliptical plate of $a/b=5$ with respect to n	20

Figure 3.8.	Convergence of the deflection parameter $w_{max}(D/q_0)$ of clamped super elliptical plate of $a/b=20$ with respect to	20
Figure 3.9.	The geometry of the super ellipses that are examined for corner forces.....	24
Figure 3.10.	The variation of the bending moment at the corners of the super ellipses with respect to	25
Figure 4.1.	Super elliptical plate edges in cartesian coordinate system	27
Figure 4.2.	Change of the frequency parameter λ^2 of a simply supported super elliptical plate of $n=1$ with respect	44
Figure 4.3.	Change of the frequency parameter λ^2 of a simply supported super elliptical plate of $n=10$ with respect to ν	44
Figure 5.1.	Through-the-thickness distribution of the volume fraction of the ceramic	46
Figure 5.2.	Maximum static deflections of the super elliptical plates of $n=1$ (elliptical).....	51
Figure 5.3.	Maximum static deflections of the super elliptical plates of $n=4$	51
Figure 5.4.	Maximum static deflections of the super elliptical plates of $n=10$	52

LIST OF TABLES

Table 3.1.	The calculated perimeter and area of the super ellipses for $a=1$, and $b=1$	14
Table 3.2.	Deflection parameters $w_{max}(D/q_0)$ for clamped super elliptical plates obtained by the trial function of $r=2$	15
Table 3.3.	Deflection parameters $w_{max}(D/q_0)$ for clamped super elliptical plates obtained by the trial function of $r=4$	16
Table 3.4.	Deflection parameters $w_{max}(D/q_0)$ for clamped super elliptical plates obtained by the trial function of $r=6$	17
Table 3.5.	Deflection parameters $w_{max}(D/q_0)$ for clamped super elliptical plates obtained by the trial function of $r=8$	18
Table 3.6.	Bending moments for two types of the plates at $x=0$ and $y=0$	23
Table 3.7.	The coordinates of the points checked for bending moments and the corresponding bending moment parameters	25
Table 4.1.	Comparison of the frequency parameters ($\lambda^2 = \omega(b^2 \sqrt{\rho h / D})$) with previously obtained results.....	33
Table 4.2.	Frequency parameters for a simply supported super elliptical plate of [n=1].....	34
Table 4.3.	Frequency parameters for a simply supported super elliptical plate of [n=2].....	35

Table 4.4.	Frequency parameters for a simply supported super elliptical plate of [n=3].....	36
Table 4.5.	Frequency parameters for a simply supported super elliptical plate of [n=4].....	37
Table 4.6.	Frequency parameters for a simply supported super elliptical plate of [n=5].....	38
Table 4.7.	Frequency parameters for a simply supported super elliptical plate of [n=6].....	39
Table 4.8.	Frequency parameters for a simply supported super elliptical plate of [n=7].....	40
Table 4.9.	Frequency parameters for a simply supported super elliptical plate of [n=8].....	41
Table 4.10.	Frequency parameters for a simply supported super elliptical plate of [n=9].....	42
Table 4.11.	Frequency parameters for a simply supported super elliptical plate of [n=10].....	43
Table 5.1.	Comparison of the displacement parameter ($\lambda=w_{max}(D/q_0)$,) with previously obtained results.....	51
Table 6.1.	Frequency parameters, $10^4 \omega b^2/h$, for simply supported super elliptical plates made of ceramic	55
Table 6.2.	Frequency parameters, $10^4 \omega b^2/h$, for simply supported super elliptical plates which have material composition of N=0.1	56

Table 6.3.	Frequency parameters, $10^4 \omega b^2/h$, for simply supported super elliptical plates which have material composition of $N=0.5$	56
Table 6.4.	Frequency parameters, $10^4 \omega b^2/h$, for simply supported super elliptical plates which have material composition of $N=1$	57
Table 6.5.	Frequency parameters, $10^4 \omega b^2/h$, for simply supported super elliptical plates which have material composition of $N=5$	57
Table 6.6.	Frequency parameters, $10^4 \omega b^2/h$, for simply supported super elliptical plates which have material composition of $N=15$	58
Table 6.7.	Frequency parameters, $10^4 \omega b^2/h$, for simply supported super elliptical plates made of metal.....	58

LIST OF SYMBOLS

D	Bending rigidity of the plate
E	Young's modulus of the plate material
E_{eff}	Effective Young's modulus
h	Plate thickness
m_x	Bending moment in x direction
m_y	Bending moment in y direction
N	Power law exponent
n	Super elliptical power
P_{eff}	Any effective material property
P_{bot}	Material properties of the bottom surface material
P_{top}	Material properties of the top surface material
q_0	Uniformly distributed surface load of the plate
r	Order of the polynomial trial function
s	Riemann sum
T	Kinetic energy of the plate
T_{max}	Maximum kinetic energy of the plate
U	Strain energy of the plate
u	Displacement component along the x, direction
U_{max}	Maximum strain energy of the plate
v	Displacement component along the y direction
V_{bot}	Volume fraction of the bottom surface material
$V(z)$	Volume fraction
V_{top}	Volume fraction of the top surface material
w	Displacement component along the z direction
w_0	Transverse deflection of a point on the middle surface of plate
$W(x,y)$	Shape function
α_i	Unknown coefficients
α_{ij}	Unknown coefficients

Δ	Displacement parameter
∇^2	Laplace operator
∇^4	Biharmonic operator
δu	A small virtual displacement in x direction
δv	A small virtual displacement in y direction
δw	A small virtual displacement in z direction
ε_x	Strain in x direction
ε_y	Strain in y direction
λ	Displacement parameter
λ^2	Frequency parameter of the plate
ν	Poisson ratio of the plate material
ν_{eff}	Effective Poisson's ratio
ω	Natural circular frequency of the plate
Π	Total potential energy of the plate
ρ	Material density
ρ_{eff}	Effective mass per unit area
$\bar{\rho}_{\text{eff}}$	Effective mass density
σ_x	Stress in x direction
σ_y	Stress in y direction

STATICS AND DYNAMICS OF SUPER ELLIPTICAL HOMOGENEOUS AND FGM PLATES

1. INTRODUCTION

Super elliptical plates can be identified with the super elliptical boundary shape. This class of plates includes a wide range of geometrical shapes. These plates, which are defined by shapes between an ellipse and a rectangle, have a wide range of use in engineering applications. Although they do not have sufficient engineering data for the types of the super elliptical plates that approach to a rectangle with rounded corners, this sort of plates are extensively used as structural and machine elements, [1]. They have a broad area of use in mechanical, civil, aerospace and many other engineering branches, but they do not have sufficient engineering data as declared by references [1-2].

1.1. Homogeneous Plates

The studies on bending of plates are concentrated on rectangular, circular, and elliptical plates which can be considered as extreme cases of super elliptical plates [3-11]. Mohr [3] used a least squares approach to obtain polynomial solutions for the deflected shape of thin plates in flexure. He worked on triangular and rectangular plates for clamped and simply supported boundary conditions. The obtained solutions are in good agreement with exact values which are also presented in reference [3]. Muhammad and Singh [5] worked on a finite element solution for bending of rectangular, circular, elliptic and skew plates. They used first order shear deformable plate model and obtained solutions for both clamped and simply supported plates. They also studied on plates having openings. They presented their results for different solution levels and compared them with known exact values. Korol [6] worked on development of a technique for the solution of boundary value problems of the longitudinal transverse bending of orthotropic circular plates resting on a linearly elastic base.

Considering simply supported curved edges; ignoring the effect of Poisson's ratio which is in the strain energy expression apart from the one in the bending stiffness of the plate, leads to considerable error. Therefore, special care is taken of various Poisson's ratio values. Plate vibration studies on circular, elliptical, and rectangular shapes are extensively included in the literature [12-21], but very limited for other shapes that can be expressed by the super elliptical boundary equation.

Chakraverty et al. [13] studied free vibration of annular elliptical plates using boundary characteristic orthogonal polynomials as shape functions in the Rayleigh-Ritz method. In their work they considered combinations of simply supported, clamped, and free boundaries for inner and outer edges. They investigated the effect of boundary conditions and hole size on different modes of vibration. Leissa [12] presented a wide study on vibration of plates for many plate shapes. Chen et al. [14] employed radial basis function for free vibration analysis of clamped plates. They examined the validity of the method by rectangular and circular plates. Wang et al. [1] obtained solutions for super elliptical plates by using two dimensional polynomials at degree of 12 for frequency and buckling factors. Although they worked on a wide range of this class of plates, they neglected the effect of Poisson's ratio on the behavior of simply supported plates. Zhou et al. [22] analyzed the three dimensional free vibration of super elliptical plates by Ritz method. They studied the effect of geometric parameters on vibration behavior of the super elliptical plates with free and fixed perimeters. Altekin [2] studied on the static and dynamic behavior of super elliptical plates. He used both variational and weighted residual methods and compared the results. He did not study on the vibration of simply supported plates. He studied the vibration problem as specifically valued cases. In the current study the vibration problem is approached parametrically.

Tezcan [23] presented the framework method for nonlinear analysis of thin plates. He idealized the plate into a grid framework of one dimensional bars and combined the cross-sectional areas of the members with the moments of inertia torsional rigidities. Muehrjee [15] extended the work on elliptical plate vibrations to the ones resting on elastic media. The author approached the solution of the integral equation of the system via orthogonal polynomials. Bayer et al. [16] considered the vibration of clamped elliptical plates with variable thickness.

They solved the partial differential equations of the plate by both moment method and Rayleigh-Ritz method and compared the results for several aspect ratios of the elliptical plates. Vibration of symmetrically laminated super elliptical plates was studied by Chen et al. [17]. The transverse shear is an important factor in the mechanical behavior of the laminated composite panels; therefore they preferred shear deformable plate model. Leissa [18], Sato [19], and Narita [20-21] obtained results for simply supported elliptical plates via several methods. They obtained frequency parameters for several values of Poisson's ratios.

1.2. Functionally Graded Material (FGM) Plates

In the literature it is seen that the studies on super elliptical plates or FGM plates are limited and the ones in the available literature are introduced here in brief. The concept of functionally graded materials was first introduced by a group of material scientists in Japan [24, 25]. The establishment of the concept of FGM originated to various research branches; thermal stress analysis, mechanical plate model applications, fracture analysis, electrical system analysis, vibration and control applications, etc. Existence of natural materials that behave like FGM is also considerable. Amada et al. [26] investigated the fiber texture of bamboo trees, and they found that the tensile strength of the bamboo's culm increases parabolically in the radial direction. They made the assumption of volume fraction rule for a natural material and compared their theoretical results with experimental ones. They concluded their study by declaring that bamboo is a structurally smart plant.

Zenkour [4] presented a two dimensional solution for bending analysis of simply supported functionally graded ceramic-metal rectangular sandwich plates. He obtained non dimensional stress solutions for plates with two different ceramic-metal mixtures. Numerical results were obtained for sinusoidal, first-order, third-order, and classical theories. The effect of material distribution on the deflections and stresses was examined. Ferreira et al. [27] studied natural frequencies of simply supported rectangular FGM plates. They considered third order shear deformation plate theory. A meshless Galerkin formulation was conducted in order to solve the partial differential equations. They employed Mori-Tanaka homogenization method to find the effective bulk modulus, and the effective shear modulus. Prakash and

Ganapathi [24] worked on the asymmetric flexural vibration and thermoelastic stability of FGM circular plates by finite element method. In that work aluminum/alumina is considered as functionally graded material for the numerical illustrations. Suresh [28] presented the wide area of use of multi-layered and graded materials, and concentrated on modeling and design guidelines.

Chi and Chung [29, 30] provided the literature an extensive study on mechanical behavior of FGM plates. They considered rectangular plates graded with power-law, sigmoid, and exponential functions. They obtained both closed form solutions and finite element solutions. Cheng and Batra [31] used Reddy's third order plate theory to study buckling and steady state vibrations of a simply supported FGM polygonal plate resting on Winkler-Pasternak elastic foundation and subjected to uniform in-plane load. The mechanical properties of the material were assumed to vary in the thickness direction. They emphasized on the analogy between plate behavior and membrane behavior.

Croce and Venini [32] contributed to static analysis of FGM Reissner-Mindlin plates with finite elements. They determined the equations governing the behavior of rectangular FGM plates using the variational approach. They determined that the response of FGM plates to thermal load does not lie between the one single-constituent homogeneous plates.

Ruys et al. [33] concentrated on experimental investigation of electrical/thermal FGM systems. Liew et al. [34] presented a finite element formulation based on a first order shear deformation theory for the active control of functionally graded material plates with integrated piezoelectric sensor/actuator layers subjected to a thermal gradient. They obtained numerical results for the control of bending and torsional deflections and vibrations for a FGM plate comprising zirconia and aluminium. He et al. [35] performed a study based on classical laminated plate theory for the shape and vibration control of FGM plates. They presented results for the composition of aluminum oxide/Ti-6Al-4V. Vel and Batra [36] presented a three-dimensional exact solution for free and forced vibrations of simply supported FGM rectangular plates. They performed studies for various volume fractions. They worked on both classical and shear deformable plate theories and pointed that the first order shear deformation

theory performs better than the third order shear deformation theory for the FGM plates that they worked on.

The influence of the constituent volume fractions and the effects of the materials on the parametric instability regions were studied by Ng et al. [37]. They studied on rectangular plates which have been most common shapes studied in the literature.

1.3. Summary of the Numerical Analyses

The first part of this study examines the bending behavior of clamped super elliptical plates under uniformly distributed surface load. The maximum displacements of a wide range of plates are tabulated. For two types of super elliptical plates the mid point moments are calculated. The effect of roundness on corner stresses is also examined. Galerkin's method with polynomial shape functions is employed for the solution of the partial differential plate equations.

The second part of this study examines angular frequencies of super elliptical plates considering sensitivities of the frequency parameters by different super ellipticity degrees, aspect ratios of the super ellipses, and Poisson's ratio of the material. The study is carried on for five Poisson's ratios (0.1, 0.2, 0.3, 0.4, and 0.5) and twenty four a/b ratios. Ritz method is used in this part. The trial functions used in the Ritz method are presented in Chapter 4.

Finally static and dynamic analyses are conducted for FGM plates. The basic idea of a FGM was to prepare a new composite by using heat resistant ceramics on the high temperature side and tough metals with high thermal conductivity on the low temperature side, with a gradual compositional variation from ceramic to metal [25]. The advanced properties of graded materials like high strength and ability to resist high temperature led to their widespread use in engineering practices. They are known to be employed as structural members in extremely high temperature environments such as nuclear reactors and high speed spacecraft industries [24]. High external loads applied to composite structure will affect its integrity; therefore it is essential to understand the mechanical behavior of an FGM plate.

2. PLATE MODEL

The two dimensional plate theories can be classified into two types:

- 1- Classical plate theory (Kirchhoff plate theory)
- 2- Shear deformation plate theories

The Kirchhoff plate theory for the pure bending case is based on the displacement field:

$$\begin{aligned}
 u(x, y, z) &= -z \frac{\partial w_0}{\partial x} \\
 v(x, y, z) &= -z \frac{\partial w_0}{\partial y} \\
 w(x, y, z) &= w_0(x, y)
 \end{aligned} \tag{2.1}$$

where u , v , and w are the displacement components along the x , y , and z directions, respectively and w_0 is the transverse deflection of a point on the middle surface. The above displacement field implies that straight lines normal to the x - y plane before deformation remain straight and normal to the middle surface after deformation. The Kirchhoff plate theory assumes that both transverse shear and transverse normal effects are neglected; which means that deformation is only caused by bending.

The shape of a plate is defined by describing the geometry of its middle surface which divides the plate thickness h into two at each point. The small deflection plate theory which is generally attributed to Kirchhoff can be summarized by the following assumptions [9]:

- 1- The material of the plate is elastic, homogeneous, and isotropic.
- 2- The bounding surfaces are flat.

- 3- The thickness of the plate is small compared to its lateral dimensions. A thickness which is less than one tenth of the small lateral dimension is considered as the limit of the small deflection theory.
- 4- The deflections are small compared to the plate thickness. A maximum deflection of one fifth of the thickness is considered as the limit for the small deflection theory.
- 5- The slopes of the middle surface are small compared to unity.
- 6- The deformations are such that, straight lines which are initially normal to the middle surface remain straight lines and normal to the middle surface. Deformations due to the transverse shear are neglected.
- 7- The deflection of the plate is produced by displacement of points of the middle surface normal to its initial plane.
- 8- The stresses normal to the middle surface are negligible.
- 9- The strains in the middle surface produced by in plane forces can be neglected in comparison with the strains due to bending.

In addition to Kirchhoff plate theory there are a number of shear deformation plate theories. The simplest is the first order shear deformation plate theory which is known as the Mindlin plate theory. The Mindlin plate theory assumes that the transverse shear strain is constant with respect to the thickness coordinate. Second and higher order shear deformation plate theories use higher order polynomials in the expansion of the displacement components through the thickness of the plate. In Fig 2.1 geometries of an edge of a plate in various plate theories are presented.

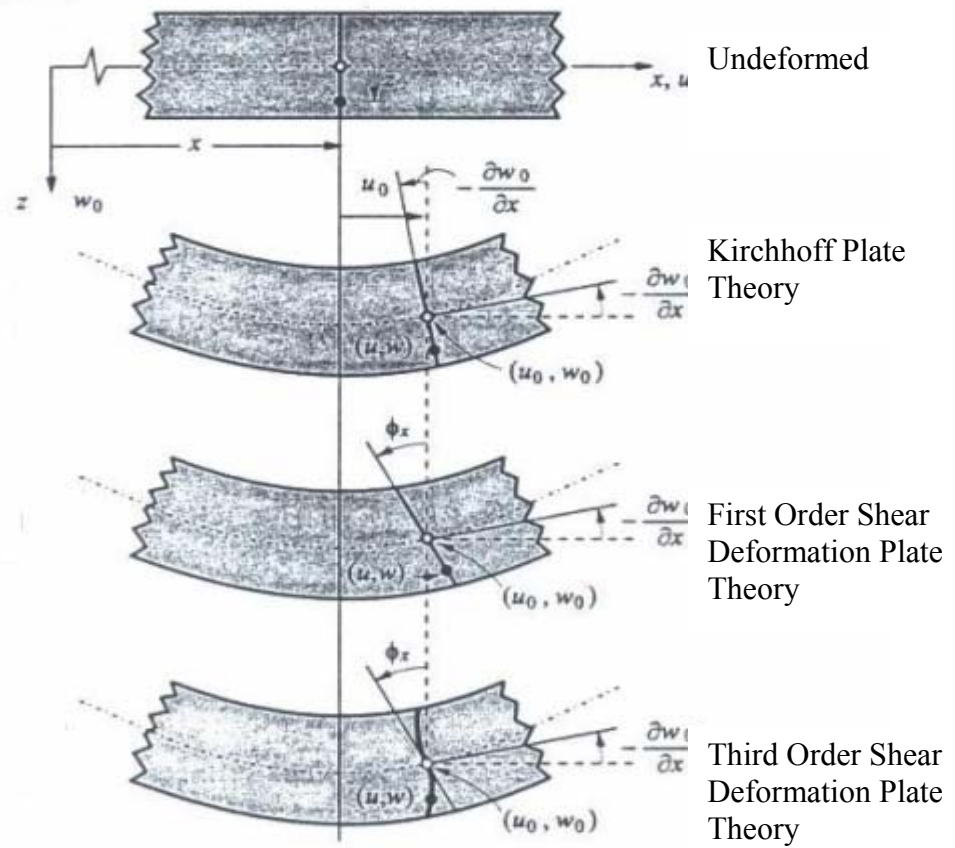


Fig 2.1. Undeformed and deformed geometries of an edge of a plate in various plate theories [8]

In addition to its inherent simplicity and low computational cost, the first order plate theory often provides a sufficiently accurate description of the global response (e.g. deflections, buckling loads, and natural vibration frequencies) for thin to moderately thick plates [8].

In this study Kirchhoff plate theory is employed.

3. STATIC ANALYSIS OF SUPER ELLIPTICAL CLAMPED PLATES BY MESHLESS GALERKIN METHOD

In this part of the study clamped super elliptical plates under uniformly distributed surface load are statically analyzed. Kirchhoff plate model is conducted for homogeneous and isotropic material. The lack of contributions on the static behavior of this sort of plate shapes is the fundamental motivation of the current study. A meshless Galerkin method is carried out to obtain solutions. The Method is conducted for polynomial series at powers ranging from 2 to 8 in order to get converging solutions. Maximum deflections of the plates are obtained and the results are arranged in tabular form. For purpose of understanding the behavior trend of the structure with respect to the parameters some of the solutions are also presented in graphical form. The study is conducted for a wide range of super elliptical plates. The results are also examined with respect to the parameters a/b ratios and n which are the plate dimension ratio and the super elliptical power respectively.

3.1. Basic Assumptions and Equations

The boundary shape equation of this class of plates can be represented by:

$$\frac{x^{2n}}{a^{2n}} + \frac{y^{2n}}{b^{2n}} = 1 \quad (3.1)$$

where n is the power of the super ellipse. The graphical representation of above boundary for $a=1$ and $b=1$ is as in Figure 3.1.

The super elliptical powers, n , are chosen from 1 to 10. For the entire study a is kept constant as 1, and b is chosen for 14 different numbers from 1 to 20 in order to obtain results for various a/b ratios.

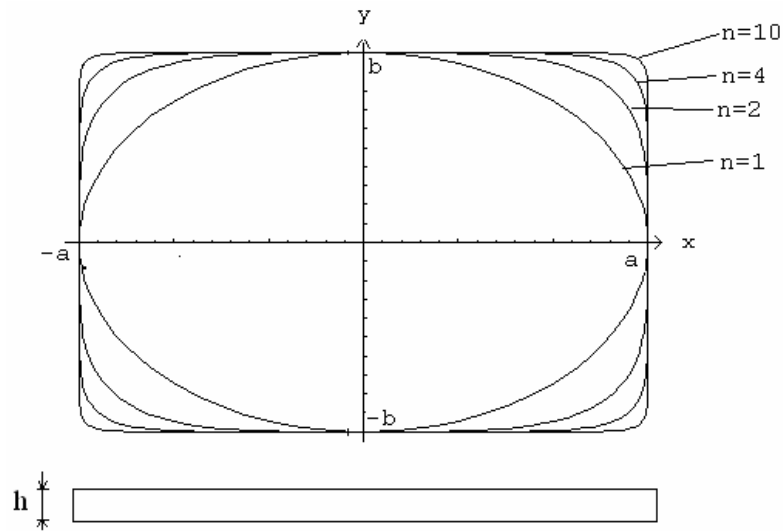


Fig.3.1. Super elliptical plates having the boundary equation $(x^{2n}/a^{2n}) + (y^{2n}/b^{2n}) = 1$.

The edges of the analyzed super ellipses are assumed to be clamped. Therefore the solution should satisfy:

$$w=0 \text{ and } \frac{\partial w}{\partial n_i} = 0 \quad (3.2)$$

at the plate edge, where n_i is the outward normal of the boundary, and w is the deflection function. In addition to the geometrical boundary conditions these kinematical boundary conditions are also satisfied by the selected trial functions. The trial functions are constructed from a complete set of polynomials in such a way that,

$$w(x, y) = \sum_i^r \sum_j^r \alpha_{ij} \left(\frac{x^{2n}}{a^{2n}} + \frac{y^{2n}}{b^{2n}} - 1 \right)^2 x^i y^j \quad (3.3)$$

and $i+j \leq r$, so r is the order of the polynomial trial function. Here α_{ij} are the undetermined coefficients. The existence of $(x^{2n}/a^{2n} + y^{2n}/b^{2n} - 1)^2$ in Eq. (3.3) guarantees that every element of these trial functions satisfy the boundary conditions of the problem. Knowing that the deflection function of the chosen system is an even function, the elements of the trial

function which has odd powers of x or y are eliminated. For example the trial function for $r=2$ is

$$\alpha_{00} \left(\frac{x^{2n}}{a^{2n}} + \frac{y^{2n}}{b^{2n}} - 1 \right)^2 x^0 y^0 + \alpha_{02} \left(\frac{x^{2n}}{a^{2n}} + \frac{y^{2n}}{b^{2n}} - 1 \right)^2 x^0 y^2 + \alpha_{20} \left(\frac{x^{2n}}{a^{2n}} + \frac{y^{2n}}{b^{2n}} - 1 \right)^2 x^2 y^0 \quad (3.4)$$

Galerkin's Method is used to obtain the solutions; therefore the partial differential equation of the uniformly loaded plates is directly used:

$$\frac{\partial^4 w}{\partial x^4} + 2 \frac{\partial^4 w}{\partial x^2 \partial y^2} + \frac{\partial^4 w}{\partial y^4} = \frac{q_0}{D} \quad (3.5)$$

where q_0 is the uniformly distributed surface load of the plate and D is the bending rigidity of the plate which is:

$$D = \frac{Eh^3}{12(1-\nu^2)} \quad (3.6)$$

Here E is Young's modulus of the plate material, h is the plate thickness, and ν is the Poisson ratio of the plate material. . Eq. (5) can also be represented in terms of biharmonic operator ∇^4 .

$$\nabla^4 w - \frac{q_0}{D} = 0 \quad (3.7)$$

3.2. Solution by Galerkin's Method

Galerkin's method has been used to solve problems in structural mechanics, dynamics, fluid flow, heat and mass transfer, etc. Problems governed by ordinary differential equations or partial differential equations have been investigated by Galerkin formulations. The method

is proved to provide solutions of significant accuracy with minimal manual effort and computer execution time for various problems [38-40].

Since the virtual work of internal forces is obtained directly from the differential equations without determining the strain energy this method appears to be more practical than variational methods. Accuracy of the method depends on the selected shape function. Solutions can be obtained by satisfying only the geometrical boundary conditions of the problem by the assumed series expression of the plate surface, but the solution converges much faster when all the boundary conditions are satisfied.

Galerkin's method can be applied to small and large deflection theories, linear and nonlinear problems of plates provided that differential equations of the problem under investigation have already been determined. In order to deal with the plate bending problem a complete set of independent, continuous functions which are capable of representing the plate deflection are selected.

$$w(x, y) = \sum_{i=1}^n \alpha_i f_i(x, y) \quad (3.8)$$

Each term of this expression must satisfy all boundary conditions of the problem. Since the governing differential equation of plates subjected to lateral load q_0 is based on the equilibrium of the internal and external forces in the z direction, the total work, performed by all these forces, during a small virtual δw displacement can be expressed by

$$\iint_A (\nabla^4 w - \frac{q_0}{D}) \delta w dx dy = 0 \quad (3.9)$$

This equation represents the basic variational equation of plate bending. Substituting this expression into Eq. (3.8) gives

$$\sum_{i=1}^n \delta c_i \iint_A \left[\nabla^4 w(x, y) - \frac{q_0}{D} \right] \alpha_i f_i(x, y) dx dy = 0 \quad (3.10)$$

Eq. (3.10) must be satisfied for any values of δc_i , and it follows that

$$\begin{aligned} \iint_A \left(\nabla^4 w - \frac{q_0}{D} \right) \alpha_1 f_1(x, y) dx dy &= 0 \\ \iint_A \left(\nabla^4 w - \frac{q_0}{D} \right) \alpha_2 f_2(x, y) dx dy &= 0 \\ \dots\dots\dots \\ \iint_A \left(\nabla^4 w - \frac{q_0}{D} \right) \alpha_n f_n(x, y) dx dy &= 0 \end{aligned} \quad (3.11)$$

The integrals are evaluated over the entire surface of the plate. In this way the solution of the differential equation of the plate is reduced to the evaluation of definite integrals of simple functions. After the evaluation of the integrals a set of linear equations is obtained. The number of equations is equal to the number of unknown coefficients α_i in the expression (3.8), and then the displacement function is obtained.

3.3. Integration over the Super Elliptical Region

During solutions of differential equations with approximate methods there are difficulties arising from integration over a super elliptical area. Any deviation from the area of the super ellipse will cause extra error in the results. Calculating the area and perimeter of the region may give an idea about the convergence of the integration. Therefore the areas and perimeters of the super ellipses are calculated for $a=1$ and $b=1$. The super elliptical function becomes:

$$x^{2n} + y^{2n} - 1 = 0 \quad (3.12)$$

$$y = \sqrt[2n]{1-x^{2n}} \quad (3.13)$$

and

$$y' = -x^{-1+2n}(1-x^{2n})^{-1+\frac{1}{2n}} \quad (3.14)$$

Thus, calculation of the Riemann sum, as

$$s \approx \sum_{i=1}^n \sqrt{1+y'^2} \Delta x \quad (3.15)$$

will give the length of any curve. In that case the exact value of the perimeter should be expected for $n=1$.

The shapes of the super ellipses for $n=1$ and $n=10$ are a circle with a radius of 1 and a shape close to a square with an edge length of 2, respectively. The results obtained are as expected and are shown in Table 3.1.

Table 3.1. The calculated perimeter and area of the super ellipses for $a=1$, and $b=1$

n	Perimeter	Area
1	6.28318	3.141593
2	7.01768	3.496077
3	7.31776	3.642976
4	7.47984	3.723496
5	7.58144	3.774362
6	7.65096	3.809415
7	7.69319	3.835038
8	7.73736	3.854586
9	7.76348	3.869992
10	7.78092	3.882445

3.4. Presentation of the Results

Four different shape functions are used which are namely the expansions of Eq. (3.3) for $r=2, 4, 6,$ and 8 . For $n=1$ which corresponds to the elliptical boundary, by all of the shape functions exact result is obtained which is

$$w(x, y) = \left(\frac{x^2}{a^2} + \frac{y^2}{b^2} - 1\right)^2 \frac{a^4 b^4 q_0}{8(3a^4 + 2a^2 b^2 + 3b^4)D} \quad (3.16)$$

Therefore the first column ($n=1$) of the Tables 3.2-3.5 is exact and can be extended for any combination of a and b . The results which obtained pertinent to the selected trial functions are tabulated in terms of $w_{max}(D/q_0)$. Examining the results with respect to the super elliptic power n it is seen that the results diverge with increasing n . If the order of the polynomial trial function is increased the converged results are obtained for higher orders of n . Another noticeable trend is that with increasing a/b ratios the $w_{max}(D/q_0)$ values remain almost unchanged. This should be expected because of the similar geometrical shapes.

Table 3.2. Deflection parameters $w_{max}(D/q_0)$ for clamped super elliptical plates obtained by the trial function of $r=2$

a/b	$n=1$	$n=2$	$n=4$	$n=6$	$n=8$	$n=10$
1	0.01563	0.01375	0.00696	0.00335	0.00172	0.00096
1.2	0.02142	0.01873	0.00953	0.00463	0.00240	0.00135
1.4	0.02603	0.02245	0.01157	0.00577	0.00306	0.00175
1.6	0.02949	0.02501	0.01314	0.00680	0.00372	0.00218
1.8	0.03203	0.02671	0.01436	0.00776	0.00441	0.00266
2	0.03390	0.02783	0.01531	0.00864	0.00512	0.00319
3	0.03835	0.02983	0.01778	0.01167	0.00813	0.00587
4	0.03985	0.03027	0.01856	0.01282	0.00953	0.00739
5	0.04052	0.03045	0.01885	0.01325	0.01007	0.00802
7	0.04109	0.03060	0.01905	0.01351	0.01040	0.00842
9	0.04132	0.03066	0.01912	0.01359	0.01049	0.00852
10	0.04139	0.03068	0.01914	0.01361	0.01051	0.00854
15	0.04154	0.03072	0.01917	0.01364	0.01055	0.00858
20	0.04160	0.03074	0.01918	0.01365	0.01056	0.00859

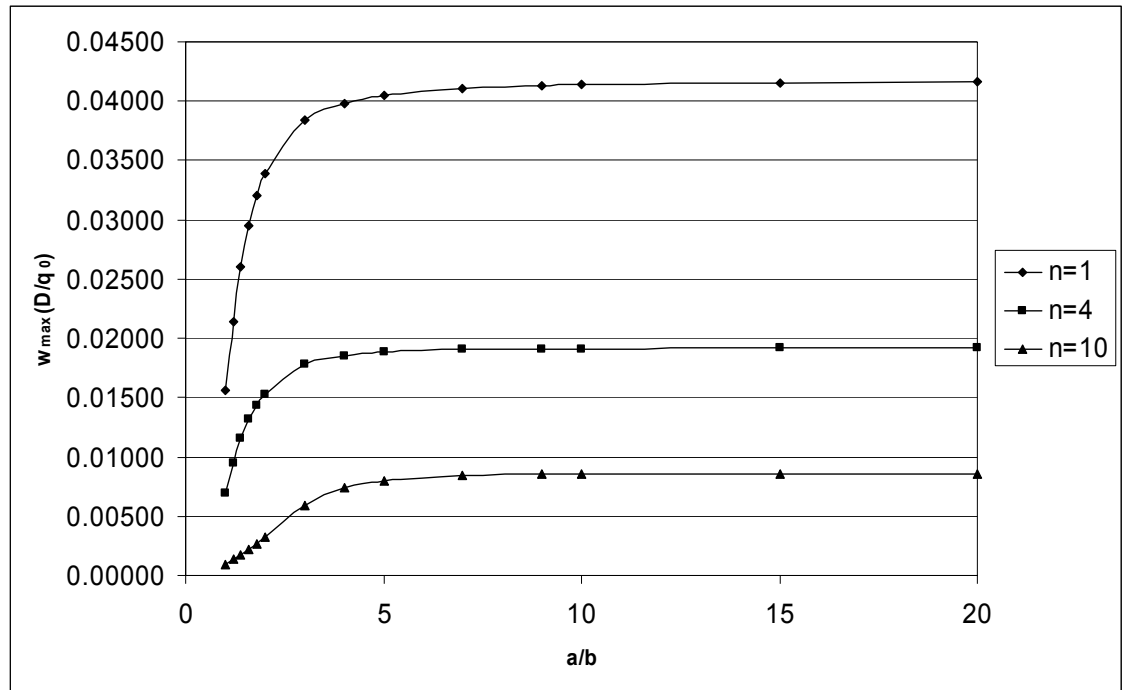


Fig. 3.2. Change of the deflection parameter $w_{max}(D/q_0)$ of clamped super elliptical plate obtained by the trial function of $r=2$ with respect to a/b ratio

Table 3.3. Deflection parameters $w_{max}(D/q_0)$ for clamped super elliptical plates obtained by the trial function of $r=4$

a/b	n=1	n=2	n=4	n=6	n=8	n=10
1	0.01563	0.01817	0.01683	0.01404	0.01129	0.00900
1.2	0.02142	0.02478	0.02302	0.01932	0.01563	0.01253
1.4	0.02603	0.02975	0.02785	0.02368	0.01946	0.01581
1.6	0.02949	0.03317	0.03137	0.02714	0.02274	0.01881
1.8	0.03203	0.03540	0.03386	0.02985	0.02552	0.02152
2	0.03390	0.03682	0.03562	0.03198	0.02785	0.02391
3	0.03835	0.03891	0.03919	0.03747	0.03460	0.03139
4	0.03985	0.03908	0.03990	0.03929	0.03744	0.03493
5	0.04052	0.03910	0.04007	0.04004	0.03896	0.03717
7	0.04109	0.03910	0.04016	0.04060	0.04035	0.03962
9	0.04132	0.03910	0.04021	0.04080	0.04086	0.04060
10	0.04139	0.03910	0.04022	0.04085	0.04099	0.04085
15	0.04154	0.03910	0.04026	0.04097	0.04125	0.04133
20	0.04160	0.03910	0.04027	0.04101	0.04133	0.04146

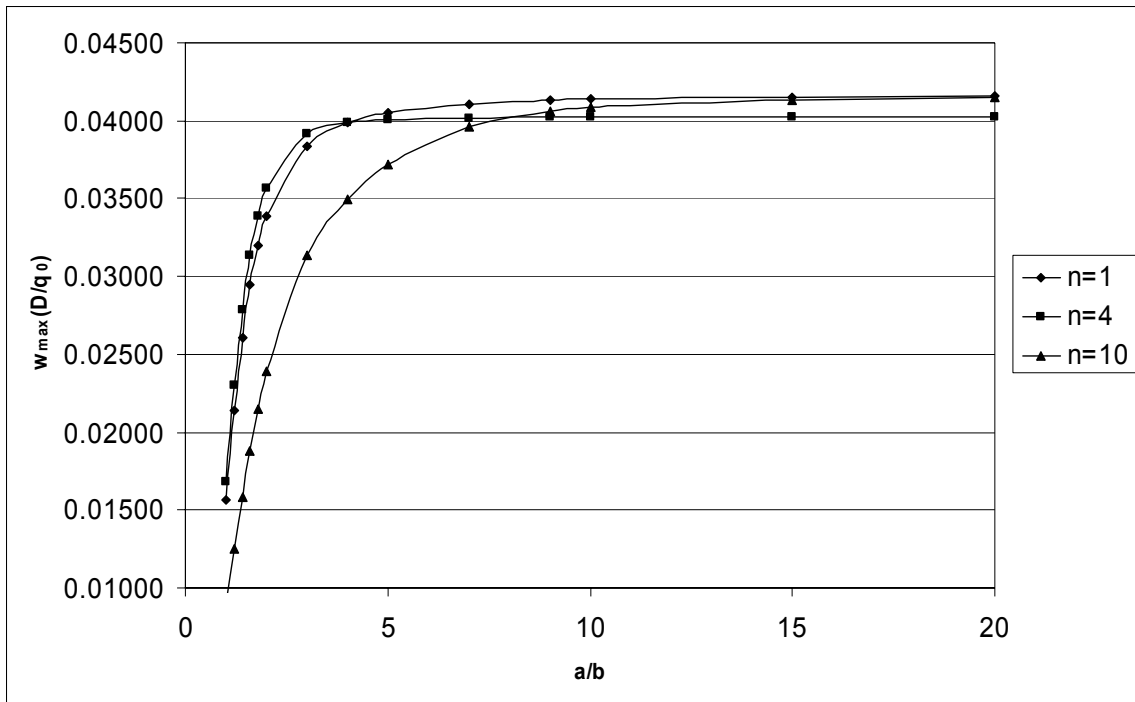


Fig. 3.3. Change of the deflection parameter $w_{max}(D/q_0)$ of clamped super elliptical plate obtained by the trial function of $r=4$ with respect to a/b ratio

Table 3.4. Deflection parameters $w_{max}(D/q_0)$ for clamped super elliptical plates obtained by the trial function of $r=6$

a/b	$n=1$	$n=2$	$n=4$	$n=6$	$n=8$	$n=10$
1	0.01563	0.01945	0.02009	0.01991	0.01964	0.01934
1.2	0.02142	0.02652	0.02740	0.02719	0.02685	0.02647
1.4	0.02603	0.03183	0.03292	0.03275	0.03243	0.03204
1.6	0.02949	0.03548	0.03672	0.03666	0.03644	0.03611
1.8	0.03203	0.03781	0.03919	0.03929	0.03921	0.03900
2	0.03390	0.03927	0.04073	0.04101	0.04110	0.04102
3	0.03835	0.04116	0.04251	0.04338	0.04411	0.04462
4	0.03985	0.04119	0.04206	0.04289	0.04380	0.04459
5	0.04052	0.04117	0.04167	0.04226	0.04314	0.04403
7	0.04109	0.04116	0.04130	0.04148	0.04209	0.04289
9	0.04132	0.04116	0.04116	0.04110	0.04144	0.04201
10	0.04139	0.04116	0.04112	0.04099	0.04123	0.04169
15	0.04154	0.04116	0.04101	0.04073	0.04075	0.04093
20	0.04160	0.04116	0.04097	0.04064	0.04061	0.04070

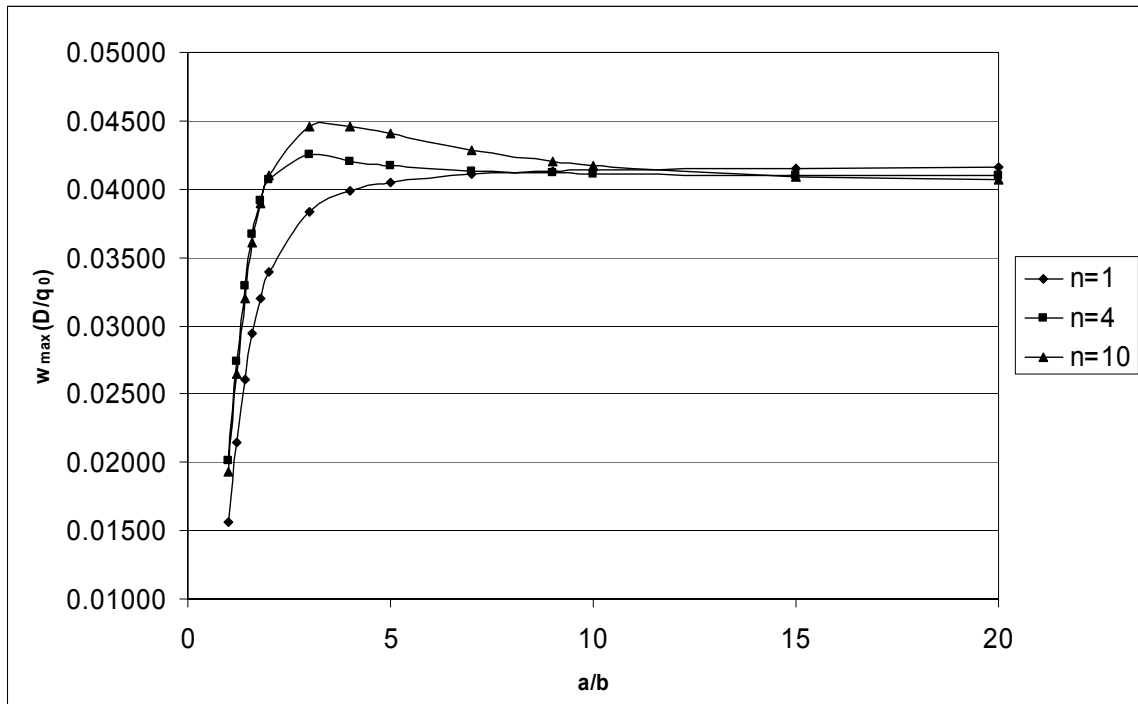


Fig. 3.4. Change of the deflection parameter $w_{max}(D/q_0)$ of clamped super elliptical plate obtained by the trial function of $r=6$ with respect to a/b ratio

Table 3.5. Deflection parameters $w_{max}(D/q_0)$ for clamped super elliptical plates obtained by the trial function of $r=8$

a/b	$n=1$	$n=2$	$n=4$	$n=6$	$n=8$	$n=10$
1	0.01563	0.01971	0.02027	0.02024	0.02019	0.02017
1.2	0.02142	0.02688	0.027632	0.02759	0.02754	0.02751
1.4	0.02603	0.03225	0.033137	0.03310	0.033048	0.03303
1.6	0.02949	0.03591	0.036861	0.03684	0.03680	0.03678
1.8	0.03203	0.03827	0.039219	0.03921	0.03918	0.03919
2	0.03390	0.03973	0.04063	0.04063	0.04062	0.04064
3	0.03835	0.04157	0.04198	0.04191	0.04124	0.04189
4	0.03985	0.04160	0.04174	0.04147	0.04186	0.04115
5	0.04052	0.04159	0.04172	0.04138	0.04100	0.04076
7	0.04109	0.04159	0.04192	0.04166	0.04119	0.04075
9	0.04132	0.04159	0.04207	0.04198	0.04157	0.04109
10	0.04139	0.04158	0.04212	0.04211	0.04175	0.04129
15	0.04154	0.04074	0.04225	0.04246	0.04232	0.04204
20	0.04160	0.04022	0.04230	0.04259	0.04254	0.04237

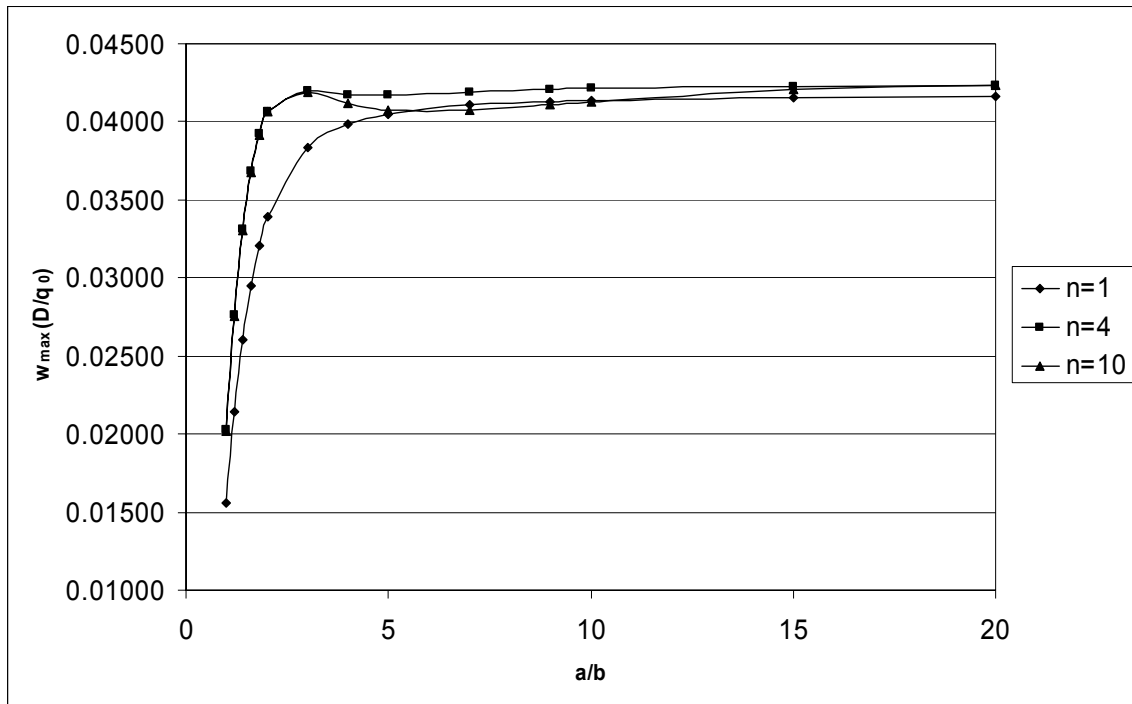


Fig. 3.5. Change of the deflection parameter $w_{max}(D/q_0)$ of clamped super elliptical plate obtained by the trial function of $r=8$ with respect to a/b ratio

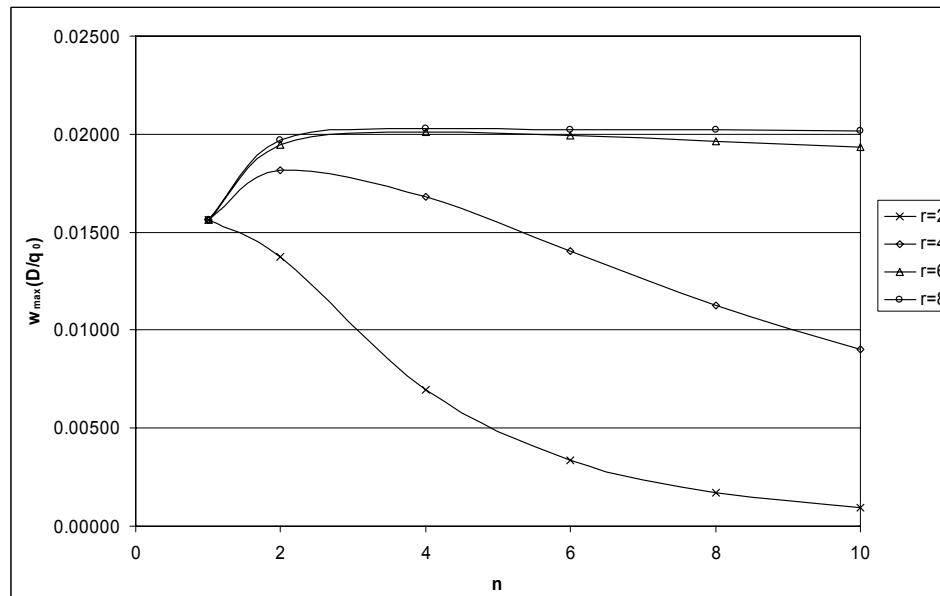


Fig. 3.6. Convergence of the deflection parameter $w_{max}(D/q_0)$ of clamped super elliptical plate of $a/b=1$ with respect to n

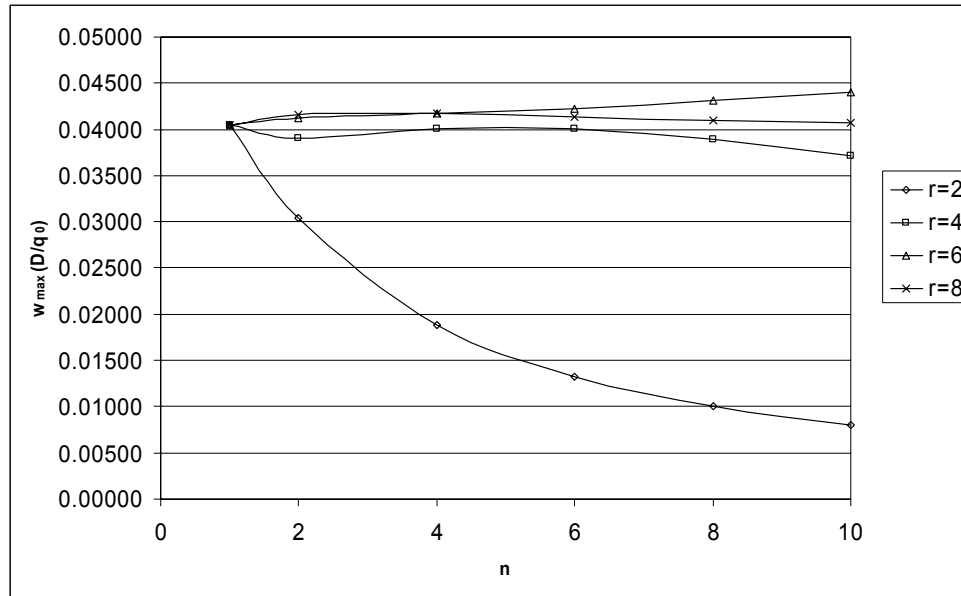


Fig. 3.7. Convergence of the deflection parameter $w_{max}(D/q_0)$ of clamped super elliptical plate of $a/b=5$ with respect to n

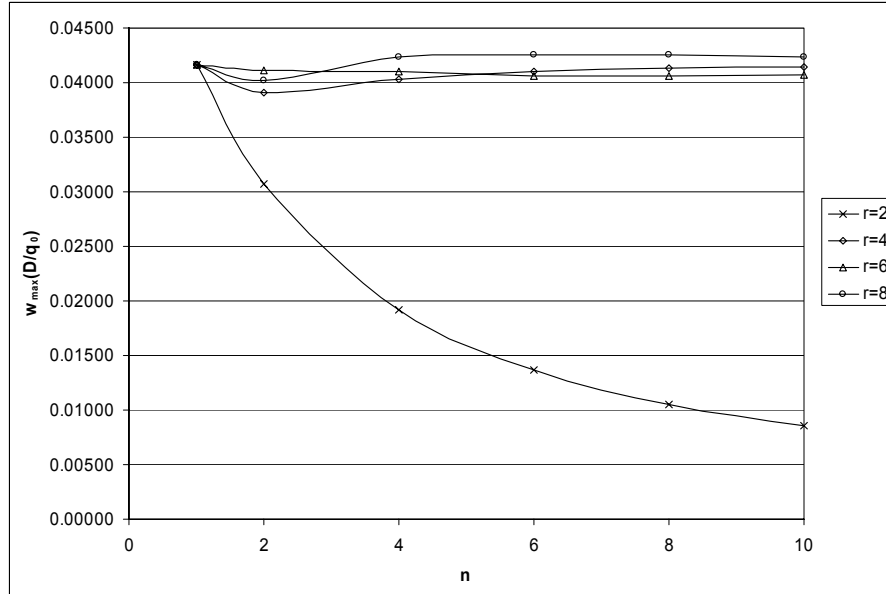


Fig.3.8. Convergence of the deflection parameter $w_{max}(D/q_0)$ of clamped super elliptical plate of $a/b=20$ with respect to n

3.5 Comparison of Results

In this study the column of $n=10$ of Table 3.5 represents the results for the shape nearest to a rectangle. The parameter value 0.02017 is in good agreement with the values presented in references [7] and [11] which are 0.02067 and 0.0202 respectively. The values obtained for ellipses (The column for $n=1$ of Tables 3.2-3.5) including circle are exact and agree with the result in reference [7] which is obtained by Ritz method.

3.6. Relation between Internal Forces and Displacements

From Hook's law the stress-strain relationships can be obtained as:

$$\sigma_x = \frac{E}{1-\nu^2} (\varepsilon_x + \nu \varepsilon_y) \quad (3.17)$$

$$\sigma_y = \frac{E}{1-\nu^2} (\varepsilon_y + \nu \varepsilon_x) \quad (3.18)$$

The strains of the plate can be introduced as $\varepsilon_x = -z \frac{\partial^2 w}{\partial x^2}$ and $\varepsilon_y = -z \frac{\partial^2 w}{\partial y^2}$ (3.19)

$$\sigma_x = -\frac{Ez}{1-\nu^2} \left(\frac{\partial^2 w}{\partial x^2} + \nu \frac{\partial^2 w}{\partial y^2} \right) \quad (3.20)$$

$$\sigma_y = -\frac{Ez}{1-\nu^2} \left(\frac{\partial^2 w}{\partial y^2} + \nu \frac{\partial^2 w}{\partial x^2} \right) \quad (3.21)$$

The sum of these stress components on the plate cross section produce the bending moments.

$$M_x = \int_{-\frac{h}{2}}^{+\frac{h}{2}} \sigma_x z dz \quad \text{and} \quad M_y = \int_{-\frac{h}{2}}^{+\frac{h}{2}} \sigma_y z dz \quad (3.22)$$

or in terms of deflections

$$M_x = \int_{-\frac{h}{2}}^{+\frac{h}{2}} -\frac{Ez}{1-\nu^2} \left(\frac{\partial^2 w}{\partial x^2} + \nu \frac{\partial^2 w}{\partial y^2} \right) z dz \quad \text{and} \quad M_y = \int_{-\frac{h}{2}}^{+\frac{h}{2}} -\frac{Ez}{1-\nu^2} \left(\frac{\partial^2 w}{\partial y^2} + \nu \frac{\partial^2 w}{\partial x^2} \right) z dz \quad (3.23)$$

$$M_x = -\frac{Eh^3}{12(1-\nu^2)} \left(\frac{\partial^2 w}{\partial x^2} + \nu \frac{\partial^2 w}{\partial y^2} \right) = -D \left(\frac{\partial^2 w}{\partial x^2} + \nu \frac{\partial^2 w}{\partial y^2} \right) \quad (3.24)$$

and

$$M_y = -\frac{Eh^3}{12(1-\nu^2)} \left(\frac{\partial^2 w}{\partial y^2} + \nu \frac{\partial^2 w}{\partial x^2} \right) = -D \left(\frac{\partial^2 w}{\partial y^2} + \nu \frac{\partial^2 w}{\partial x^2} \right) \quad (3.25)$$

Once the deflections are driven the internal forces can be obtained from them. The bending moments of two types of super elliptical plates ($n=1$ and $n=10$) are obtained with the shape function of $r=8$ and for $\nu=0.3$. The moments are evaluated for the mid-points ($x=0$ and $y=0$) of the plates. The results are tabulated in Table 3.6 with the ones obtained by Timoshenko and Woinowsky-Krieger [11] for rectangular plates. The values of $n=10$, which represents a shape similar to a rectangle, agree with the corresponding values of them.

For the rectangle of $a/b=1$, M_x/q_0 value is obtained as 0.0875 by finite element method with meshing of 10X10. Galerkin's method is a powerful tool for solving differential equations approximately [41, 42]. The advantages of the method are:

- It does not require a mesh generation
- It does not require approximations on the geometrical representation of the curved boundaries
- Direct use of the differential equation

Table 3.6. Bending moments for two types of the plates at $x=0$ and $y=0$

a/b	M_x/q_0		
	n=1	n=10	Rectangular *
1	0.08125	0.09089	0.0924
1.2	0.08520	0.09103	0.0912
1.4	0.08437	0.08518	0.0848
1.6	0.08146	0.07744	0.0772
1.8	0.07797	0.06999	0.0696
2	0.07458	0.06367	0.0632
3	0.06307	0.04851	-
4	0.05778	0.04597	-
5	0.05511	0.04607	-
7	0.05266	0.04681	-
9	0.05162	0.04745	-
10	0.05132	0.04775	-
15	0.05059	0.04878	-
20	0.05033	0.04918	-
∞	-	-	0.05

*Timoshenko and Woinowsky-Krieger [11]

3.7. Effect of Rounded Corners on Bending Moment Values

The reference [1] indicates that the high corner stresses are released when rounding the corners. In some critical cases this effect may be very advantageous for preferring super elliptical plates. In order to check this effect, bending moments at the corners of the super elliptical plates which have the super elliptical power, n , between 4 and 10 are determined. The study is conducted for super ellipses having the dimensions $a=b=1$. The moments are checked at the points where the super ellipses intersect with the line $y=x$, as seen in Fig. 3.9. The coordinates of these points and the corresponding bending moment parameters are tabulated in Table 3.7. It is observed that rounding the corners decreases the moments. The

moment parameter for the super ellipse of $n=10$ is 19.3 % higher than that of the super ellipse of $n=4$.

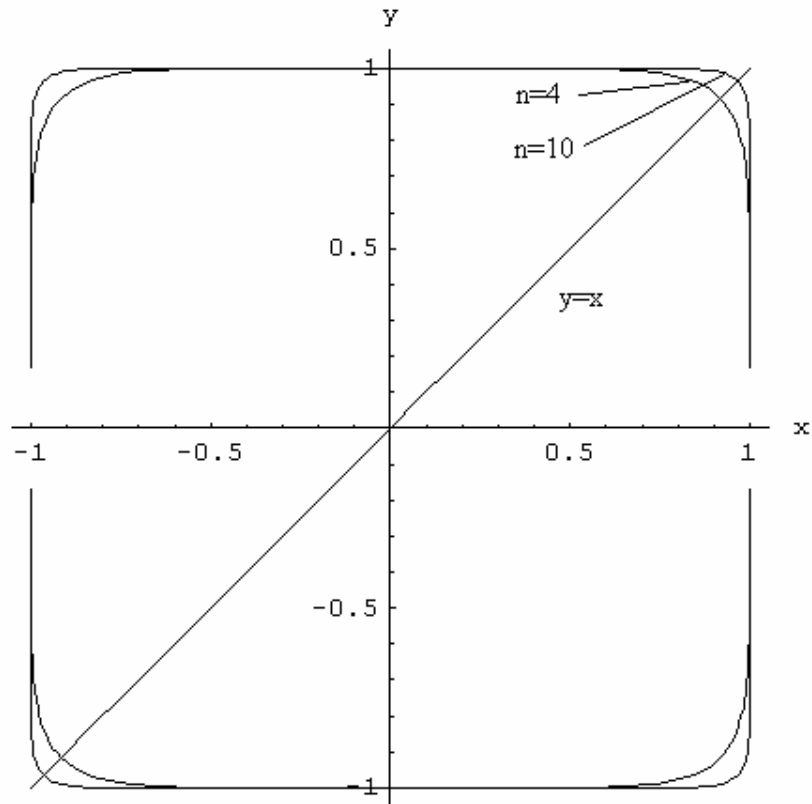


Fig. 3.9. The geometry of the super ellipses that are examined for corner forces

Table 3.7. The coordinates of the points checked for bending moments and the corresponding bending moment parameters

n	$x=y$	M_x/q_0
4	0.917	-0.0249
5	0.933	-0.0260
6	0.944	-0.0281
7	0.952	-0.0297
8	0.958	-0.0304
9	0.962	-0.0304
10	0.966	-0.0297

By decreasing super elliptical power, n , from 10 to 4 the moments also gradually decrease. At high values of n there is a small amount of decrease which may be resulted from numerical errors.

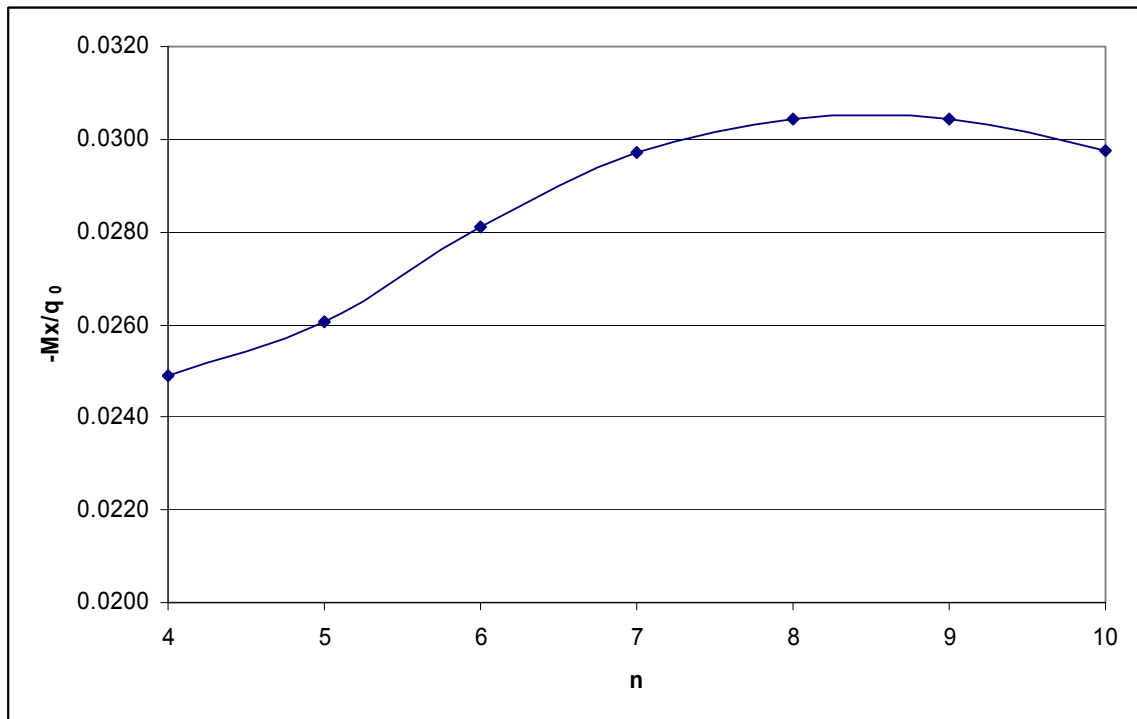


Fig 3.10. The variation of the bending moment at the corners of the super ellipses with respect to n .

4. FREE VIBRATION OF SIMPLY SUPPORTED SUPER ELLIPTICAL PLATES BY RITZ METHOD

In this part of the study the first vibration mode of simply supported super elliptical plates is discussed. This class of plates includes a wide range of external boundaries varying from an ellipse to a rectangle. Although studies on the upper and lower bounds of these plates are quite extensive, contributions on the mid shapes, especially for simply supported boundary edges, are very limited. Kirchhoff plate model with isotropic and homogeneous material is studied. The super elliptical powers are chosen from $n=1$ to 10. Ritz method is employed for the solution of the partial differential equations of the plates. The effect of Poisson's ratio, which should not be neglected for rounded edged simply supported plates, and aspect ratio of the plate dimensions are examined in details. For purpose of introducing a handy way for engineers and avoiding long computational run time, physically pertinent shape functions are utilized. The obtained angular frequency parameters are presented and compared with the parameters of the plate shapes that match the current cases which are previously obtained in the literature.

4.1. Basic Assumptions and Equations

The equation of the boundary for a super ellipse is:

$$\frac{x^{2n}}{a^{2n}} + \frac{y^{2n}}{b^{2n}} = 1 \quad (4.1)$$

where n is the power of the super ellipse. The graphical representation of the boundary of Eq. (4.1) is as in Fig. 4.1. Selection of the trial functions has crucial importance in approximation and time consuming [43, 44]. A trial function for deflection function, w , may be represented by:

$$w = \left(\frac{x^{2n}}{a^{2n}} + \frac{y^{2n}}{b^{2n}} - 1 \right) \left(\alpha_{00} + \alpha_{20} \frac{x^2}{a^2} + \alpha_{02} \frac{y^2}{b^2} \right) \quad (4.2)$$

where α_{00} , α_{20} , and α_{02} are the unknown coefficients. The chosen deflection function possesses such a property that it has the form of two-fold symmetry which is required for the fundamental vibration mode. It also satisfies the kinematic boundary condition, which is assumed as that there is no deflection at the edge of the plates.

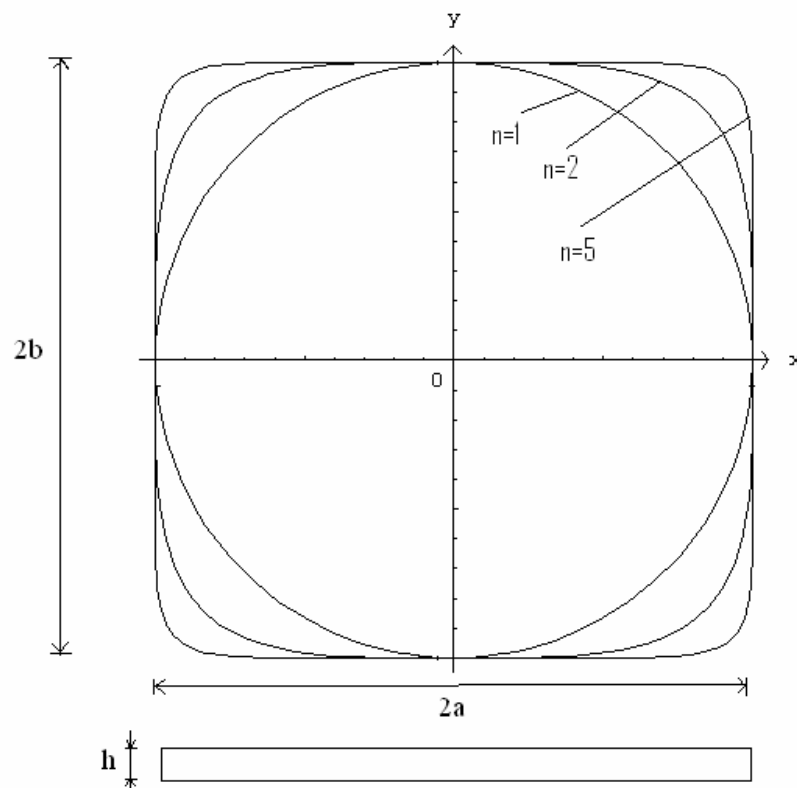


Fig. 4.1. Super elliptical plate edges in cartesian coordinate system

The expression for the strain energy of the plate is [9]:

$$U = \frac{1}{2} \iint_A D \left\{ \left(\frac{\partial^2 w}{\partial x^2} + \frac{\partial^2 w}{\partial y^2} \right)^2 - 2(1-\nu) \left[\frac{\partial^2 w}{\partial x^2} \frac{\partial^2 w}{\partial y^2} - \left(\frac{\partial^2 w}{\partial x \partial y} \right)^2 \right] \right\} dx dy \quad (4.3)$$

where $D= Eh^3/[12(1-\nu^2)]$, E is Young's modulus, and ν is Poisson's ratio. The expression representing the kinetic energy of the plate is:

$$T = \frac{1}{2} \iint_A \rho h(x, y) \left[\frac{\partial w(x, y, t)}{\partial t} \right]^2 dx dy \quad (4.4)$$

where ρ is mass density. Assuming that the plate is undergoing harmonic oscillations the lateral deflection may be written as:

$$w(x, y, t) = W(x, y) \cdot \sin(\omega t) \quad (4.5)$$

where $W(x, y)$ is the shape function and ω represents the unknown natural circular frequency of the plate pertinent to the assumed shape function. Substituting Eq. (4.5) into the expression of the kinetic energy of the oscillating plate a new expression for kinetic energy may be obtained as follows:

$$T = \frac{\omega^2}{2} \cos^2(\omega t) \iint_A \rho h(x, y) W^2(x, y) dx dy \quad (4.6)$$

The kinetic energy is at the maximum level when the velocity of the plate is maximum, which occurs when $w(x, y, t)$ is zero. This is the case when $\sin(\omega t)$ is zero, which means:

$$\omega t = n\pi \quad (n=0, 1, 2, \dots) \quad (4.7)$$

Substituting the last expression into Eq. (4.6), the kinetic energy expression becomes:

$$T = \frac{\omega^2}{2} \iint_A \rho h(x, y) W^2(x, y) dx dy \quad (4.8)$$

The strain energy is maximum when the deflection of the plate is maximum. This occurs when $\sin(\omega t)$ equals to 1. Using these values of ωt , $w(x,y,t)$ of Eq. (4.5) equals to $W(x,y)$ and the expression of maximum strain energy is identical to Eq. (4.3).

In order to apply the Ritz method firstly, an appropriate deflection shape is selected, as shown in Eq. (4.2). Then the maximum kinetic and strain energies are equated. An equation in the following form is obtained:

$$\Pi = \frac{1}{2} \iint_A D \left\{ \left(\frac{\partial^2 w}{\partial x^2} + \frac{\partial^2 w}{\partial y^2} \right)^2 - 2(1-\nu) \left[\frac{\partial^2 w}{\partial x^2} \frac{\partial^2 w}{\partial y^2} - \left(\frac{\partial^2 w}{\partial x \partial y} \right)^2 \right] \right\} dx dy - \frac{\omega^2}{2} \iint_A \rho h(x,y) w^2(x,y) dx dy = 0 \quad (4.9)$$

Eq (4.9) is minimized with respect to unknown coefficients, α_{00} , α_{20} , and α_{02} . This procedure yields a set of homogeneous linear simultaneous equations in α_i and in this way the problem is reduced to an eigenvalue problem.

4.2. Solution by Ritz Method

The objective of the variational methods is to find from a group of admissible functions those which represent the deflections of the elastic body, pertinent to its stable equilibrium condition.

The principle of minimum potential energy makes use of the change of the total potential during arbitrary variation of the deflection. Introducing δu , δv , and δw as the virtual displacements of the elastic body, the new position $(u + \delta u, v + \delta v, w + \delta w)$ produces an increase in the strain energy stored. The change in the total potential energy can be evaluated as:

$$\delta \Pi = \Pi(u + \delta u, v + \delta v, w + \delta w) - \Pi(u, v, w) \quad (4.10)$$

Since the equilibrium configuration is represented by those admissible functions which make the total potential of the system minimum, it can be stated that,

$$\delta\Pi = \delta U + \delta V = \delta(U + V) = 0 \quad (4.11)$$

Components of the compatible infinitesimal virtual displacements $(\delta u, \delta v, \delta w)$ should satisfy the geometrical boundary conditions of the elastic system, and be capable of representing all possible displacement patterns. If these admissible displacement functions are chosen properly a very good accuracy may be attained.

The Ritz method employs the principle of minimum potential energy. Of all the displacements that satisfy the boundary conditions, those making the total potential energy of the structure a minimum are the sought deflections pertinent to the stable equilibrium conditions.

The deflected middle surface may be represented in the form of a series:

$$w(x, y) = \alpha_1 f_1(x, y) + \alpha_2 f_2(x, y) + \alpha_3 f_3(x, y) + \dots + \alpha_n f_n(x, y) = \sum_{i=1}^n \alpha_i f_i(x, y) \quad (4.12)$$

where $f_i(x, y)$, $(i=1, 2, 3, \dots, n)$, are continuous functions that satisfy individually at least the geometrical boundary conditions and are capable of representing the deflected plate surface. The unknown constants $\alpha_1, \alpha_2, \alpha_3, \dots, \alpha_n$ are determined from the minimum potential energy principle as:

$$\frac{\partial E}{\partial \alpha_1} = 0, \frac{\partial E}{\partial \alpha_2} = 0, \dots, \frac{\partial E}{\partial \alpha_n} = 0 \quad (4.13)$$

With this minimization procedure, n simultaneous algebraic equations, in terms of the unknown coefficients $\alpha_1, \alpha_2, \alpha_3, \dots, \alpha_n$, will be obtained. The number of equations is equal to the number of unknown parameters, so $\alpha_1, \alpha_2, \alpha_3, \dots, \alpha_n$ can be calculated.

The potential energy of a plate from Eq (4.3) is:

$$U = \frac{1}{2} \iint_A D \left\{ \left(\frac{\partial^2 w}{\partial x^2} + \frac{\partial^2 w}{\partial y^2} \right)^2 - 2(1-\nu) \left[\frac{\partial^2 w}{\partial x^2} \frac{\partial^2 w}{\partial y^2} - \left(\frac{\partial^2 w}{\partial x \partial y} \right)^2 \right] \right\} dx dy \quad (4.14)$$

For fixed plates and simply supported plates, the second term on the right hand side of the integral expression becomes zero [7]. Thus the expression for potential energy becomes:

$$U = \frac{1}{2} \iint_A D \left\{ \left(\frac{\partial^2 w}{\partial x^2} + \frac{\partial^2 w}{\partial y^2} \right)^2 \right\} dx dy \quad (4.15)$$

The total potential energy of a plate subjected to lateral load q_0 , is expressed in the following form:

$$\Pi = \frac{1}{2} \iint_A D \left\{ \left(\frac{\partial^2 w}{\partial x^2} + \frac{\partial^2 w}{\partial y^2} \right)^2 - 2(1-\nu) \left[\frac{\partial^2 w}{\partial x^2} \frac{\partial^2 w}{\partial y^2} - \left(\frac{\partial^2 w}{\partial x \partial y} \right)^2 \right] \right\} dx dy - \iint_A w q_0 dx dy \quad (4.16)$$

The above expression may be simplified for a clamped plate as:

$$\Pi = \frac{D}{2} \iint_A \left\{ (\nabla^2 w)^2 - \frac{2q_0 w}{D} \right\} dx dy \quad (4.17)$$

For round edge plates, however, the Poisson's ratio dependent term should not be neglected. Here ∇^2 is the second order Laplace operator. In Figs. 4.2 and 4.3, the effect of Poisson's ratio on low and high ordered super ellipses is accentuated.

In order to form an expression for vibration of a plate, kinetic energy of the plate should also be identified. If the vibrating system is conservative (no energy is added or lost) the maximum kinetic energy must equal the maximum potential energy. In the case of free flexural vibration:

$$U_{\max} = T_{\max} \quad (4.18)$$

where

$$U_{\max} = \frac{1}{2} \iint_A D \left\{ \left(\frac{\partial^2 w}{\partial x^2} + \frac{\partial^2 w}{\partial y^2} \right)^2 - 2(1-\nu) \left[\frac{\partial^2 w}{\partial x^2} \frac{\partial^2 w}{\partial y^2} - \left(\frac{\partial^2 w}{\partial x \partial y} \right)^2 \right] \right\} dx dy \quad (4.19)$$

and

$$T_{\max} = \frac{1}{2} \iint_A \rho h(x, y) \left[\frac{\partial w(x, y, t)}{\partial t} \right]^2 dx dy \quad (4.20)$$

The Ritz method is conducted by minimizing the total potential energy

$$E = \frac{1}{2} \iint_A D \left\{ \left(\frac{\partial^2 w}{\partial x^2} + \frac{\partial^2 w}{\partial y^2} \right)^2 - 2(1-\nu) \left[\frac{\partial^2 w}{\partial x^2} \frac{\partial^2 w}{\partial y^2} - \left(\frac{\partial^2 w}{\partial x \partial y} \right)^2 \right] \right\} dx dy - \frac{1}{2} \iint_A \rho h(x, y) \left[\frac{\partial w(x, y, t)}{\partial t} \right]^2 dx dy \quad (4.21)$$

with respect to undetermined coefficients $\alpha_1, \alpha_2, \alpha_3, \dots, \alpha_n$.

4.3. Presentation of the Results of Dynamic Analyses

The results obtained by the various authors are presented in different parametric forms. In order to make comparison all values are normalized by the parameter $\lambda^2 = \omega(b^2 \sqrt{\rho h / D})$, which is used in the entire study. λ^2 is a multiplier of first mode frequency.

Table 4.1. Comparison of the frequency parameters ($\lambda^2 = \omega(b^2 \sqrt{\rho h / D})$) with previously obtained results

	n=1					n=8		n=10	Rectangle
	Thesis	Wang [1]	Sato [19]	Narita [20]	Leissa [9]	Thesis	Wang [1]	Thesis	Wang [1]
ν	~ 0.3	-	0.3	0.3	0.25	$\tilde{0}.3$	-	~ 0.3	-
a/b									
1	4.94058	4.935	4.935	4.935	4.865	5.0574	4.804	5.05754	4.9348
1.5	3.68719	3.681	-	-	-	3.77473	3.486	3.77521	3.56402
2	3.31446	3.303	3.293	3.303	3.172	3.40283	3.038	3.40433	3.08425
3	3.03526	3.009	-	-	3.027	3.1414	2.723	3.14575	2.74156

Table 4.2. Frequency parameters for a simply supported super elliptical plate of [n=1]

a/b	$\lambda^2 = \omega(b^2 \sqrt{\rho h / D})$					
	v=0	v = 0.1	v = 0.2	v = 0.3	v= 0.4	v = 0.5
1.0	4.44735	4.62352	4.78743	4.94058	5.08420	5.21929
1.1	4.07797	4.23634	4.38375	4.52152	4.65076	4.77236
1.2	3.82272	3.96366	4.09497	4.21781	4.33312	4.44171
1.3	3.64246	3.76706	3.88331	3.99218	4.09450	4.19096
1.4	3.51226	3.62196	3.72446	3.82060	3.91108	3.99650
1.5	3.41595	3.51229	3.60247	3.68719	3.76706	3.84257
1.6	3.34291	3.42741	3.50666	3.58126	3.65170	3.71843
1.7	3.28604	3.36014	3.42977	3.49544	3.55760	3.61659
1.8	3.24056	3.30555	3.36676	3.42463	3.47951	3.53172
1.9	3.20319	3.26024	3.31411	3.36517	3.41371	3.45999
2.0	3.17169	3.22184	3.26933	3.31446	3.35747	3.39859
2.5	3.06127	3.08862	3.11495	3.14035	3.16493	3.18875
3.0	2.98702	3.00346	3.01952	3.03526	3.05068	3.06582
3.5	2.93141	2.94244	2.95334	2.96411	2.97477	2.98531
4.0	2.88924	2.89735	2.90540	2.91340	2.92135	2.92925
4.5	2.85721	2.86356	2.86987	2.87616	2.88242	2.88866
5.0	2.83272	2.83790	2.84305	2.84818	2.85330	2.85840
6.0	2.79896	2.80265	2.80633	2.81000	2.81366	2.81730
7.0	2.77770	2.78049	2.78327	2.78604	2.78881	2.79156
8.0	2.76360	2.76578	2.76796	2.77013	2.77230	2.77446
9.0	2.75382	2.75557	2.75732	2.75907	2.76081	2.76255
10.0	2.74677	2.74821	2.74965	2.75108	2.75251	2.75394
15.0	2.72996	2.73062	2.73128	2.73194	2.73260	2.73326
20.0	2.72404	2.72442	2.72480	2.72517	2.72555	2.72593

Table 4.3. Frequency parameters for a simply supported super elliptical plate of [n=2]

a/b	$\lambda^2 = \omega(b^2 \sqrt{\rho h / D})$					
	v=0	v = 0.1	v = 0.2	v = 0.3	v= 0.4	v = 0.5
1.0	4.54268	4.71201	4.86862	5.01412	5.14985	5.27690
1.1	4.16334	4.31579	4.45682	4.58786	4.71010	4.82453
1.2	3.90020	4.03613	4.16192	4.27885	4.38795	4.49008
1.3	3.71373	3.83414	3.94563	4.04931	4.14606	4.23665
1.4	3.57871	3.68491	3.78331	3.87484	3.96029	4.04032
1.5	3.47876	3.57216	3.65875	3.73933	3.81459	3.88509
1.6	3.40304	3.48503	3.56108	3.63190	3.69806	3.76005
1.7	3.34428	3.41617	3.48289	3.54505	3.60314	3.65761
1.8	3.29754	3.36052	3.41901	3.47354	3.52453	3.57236
1.9	3.25942	3.31456	3.36582	3.41365	3.45840	3.50042
2.0	3.22754	3.27582	3.32075	3.36269	3.40199	3.43891
2.5	3.11814	3.14316	3.16661	3.18867	3.20948	3.22917
3.0	3.04540	3.05884	3.07159	3.08371	3.09526	3.10631
3.5	2.98972	2.99742	3.00482	3.01194	3.01880	3.02544
4.0	2.94611	2.95088	2.95552	2.96002	2.96441	2.96869
4.5	2.91192	2.91511	2.91823	2.92130	2.92431	2.92727
5.0	2.88504	2.88732	2.88957	2.89179	2.89398	2.89615
6.0	2.84680	2.84815	2.84950	2.85084	2.85217	2.85349
7.0	2.82193	2.82285	2.82376	2.82468	2.82559	2.82650
8.0	2.80506	2.80574	2.80641	2.80709	2.80776	2.80843
9.0	2.79317	2.79370	2.79422	2.79474	2.79527	2.79579
10.0	2.78451	2.78493	2.78535	2.78577	2.78619	2.78661
15.0	2.76351	2.76369	2.76387	2.76406	2.76424	2.76443
20.0	2.75599	2.75610	2.75620	2.75630	2.75641	2.75651

Table 4.5. Frequency parameters for a simply supported super elliptical plate of [n=4]

a/b	$\lambda^2 = \omega(b^2 \sqrt{\rho h / D})$					
	v=0	v = 0.1	v = 0.2	v = 0.3	v= 0.4	v = 0.5
1.0	4.58374	4.75088	4.90529	5.04866	5.18232	5.30742
1.1	4.20090	4.35146	4.49057	4.61972	4.74012	4.85277
1.2	3.93459	4.06910	4.19339	4.30877	4.41632	4.51691
1.3	3.74542	3.86491	3.97535	4.07786	4.17338	4.26268
1.4	3.60824	3.71401	3.81177	3.90250	3.98701	4.06597
1.5	3.50669	3.60008	3.68640	3.76650	3.84106	3.91068
1.6	3.42990	3.51223	3.58833	3.65890	3.72457	3.78583
1.7	3.37056	3.44306	3.51006	3.57217	3.62992	3.68376
1.8	3.32367	3.38746	3.44639	3.50099	3.55174	3.59901
1.9	3.28575	3.34184	3.39364	3.44162	3.48618	3.52765
2.0	3.25438	3.30366	3.34917	3.39131	3.43042	3.46680
2.5	3.14995	3.17566	3.19939	3.22134	3.24168	3.26056
3.0	3.08271	3.09613	3.10855	3.12005	3.13070	3.14060
3.5	3.03093	3.03803	3.04462	3.05073	3.05640	3.06166
4.0	2.98949	2.99332	2.99687	3.00017	3.00323	3.00607
4.5	2.95624	2.95833	2.96026	2.96206	2.96373	2.96527
5.0	2.92955	2.93069	2.93175	2.93273	2.93362	2.93445
6.0	2.89066	2.89097	2.89125	2.89149	2.89171	2.89190
7.0	2.86476	2.86479	2.86480	2.86480	2.86478	2.86475
8.0	2.84691	2.84684	2.84676	2.84667	2.84657	2.84647
9.0	2.83419	2.83408	2.83397	2.83386	2.83374	2.83362
10.0	2.82485	2.82474	2.82462	2.82450	2.82438	2.82426
15.0	2.80192	2.80184	2.80177	2.80169	2.80161	2.80154
20.0	2.79362	2.79358	2.79353	2.79348	2.79344	2.79339

Table 4.6. Frequency parameters for a simply supported super elliptical plate of [n=5]

a/b	$\lambda^2 = \omega(b^2 \sqrt{\rho h / D})$					
	v=0	v = 0.1	v = 0.2	v = 0.3	v= 0.4	v = 0.5
1.0	4.58874	4.75576	4.91009	5.05341	5.18709	5.31224
1.1	4.20557	4.35604	4.49509	4.62420	4.74461	4.85731
1.2	3.93885	4.07335	4.19765	4.31306	4.42066	4.52133
1.3	3.74928	3.86887	3.97941	4.08204	4.17767	4.26709
1.4	3.61177	3.71775	3.81571	3.90663	3.99132	4.07044
1.5	3.50998	3.60369	3.69030	3.77066	3.84546	3.91529
1.6	3.43306	3.51580	3.59226	3.66317	3.72911	3.79062
1.7	3.37369	3.44668	3.51410	3.57659	3.63466	3.68876
1.8	3.32687	3.39120	3.45061	3.50563	3.55672	3.60427
1.9	3.28912	3.34578	3.39809	3.44651	3.49142	3.53318
2.0	3.25798	3.30787	3.35391	3.39649	3.43596	3.47262
2.5	3.15543	3.18168	3.20587	3.22817	3.24878	3.26785
3.0	3.09027	3.10405	3.11673	3.12841	3.13919	3.14912
3.5	3.04014	3.04740	3.05408	3.06023	3.06589	3.07109
4.0	2.99982	3.00367	3.00720	3.01044	3.01340	3.01611
4.5	2.96726	2.96928	2.97113	2.97281	2.97434	2.97571
5.0	2.94097	2.94201	2.94294	2.94377	2.94450	2.94515
6.0	2.90242	2.90259	2.90272	2.90281	2.90286	2.90287
7.0	2.87657	2.87646	2.87633	2.87618	2.87602	2.87584
8.0	2.85867	2.85848	2.85827	2.85806	2.85784	2.85761
9.0	2.84588	2.84567	2.84545	2.84523	2.84500	2.84477
10.0	2.83646	2.83626	2.83606	2.83585	2.83563	2.83542
15.0	2.81328	2.81316	2.81304	2.81291	2.81279	2.81267
20.0	2.80487	2.80480	2.80472	2.80465	2.80457	2.80450

Table 4.7. Frequency parameters for a simply supported super elliptical plate of [n=6]

a/b	$\lambda^2 = \omega(b^2 \sqrt{\rho h / D})$					
	v=0	v = 0.1	v = 0.2	v = 0.3	v= 0.4	v = 0.5
1.0	4.59092	4.75795	4.91234	5.05575	5.18955	5.31486
1.1	4.20763	4.35813	4.49723	4.62644	4.74696	4.85981
1.2	3.94071	4.07529	4.19969	4.31523	4.42297	4.52381
1.3	3.75092	3.87067	3.98137	4.08417	4.17999	4.26961
1.4	3.61322	3.71943	3.81763	3.90878	3.99370	4.07305
1.5	3.51129	3.60531	3.69223	3.77287	3.84794	3.91802
1.6	3.43430	3.51742	3.59424	3.66548	3.73173	3.79352
1.7	3.37495	3.44836	3.51619	3.57905	3.63745	3.69185
1.8	3.32821	3.39301	3.45285	3.50827	3.55971	3.60757
1.9	3.29059	3.34777	3.40054	3.44936	3.49464	3.53671
2.0	3.25966	3.31007	3.35658	3.39958	3.43942	3.47638
2.5	3.15861	3.18535	3.20996	3.23263	3.25354	3.27283
3.0	3.09514	3.10926	3.12223	3.13414	3.14509	3.15515
3.5	3.04639	3.05384	3.06067	3.06693	3.07266	3.07789
4.0	3.00703	3.01096	3.01454	3.01780	3.02077	3.02345
4.5	2.97509	2.97713	2.97897	2.98062	2.98210	2.98341
5.0	2.94920	2.95020	2.95108	2.95186	2.95252	2.95309
6.0	2.91102	2.91112	2.91118	2.91119	2.91116	2.91108
7.0	2.88529	2.88511	2.88491	2.88468	2.88444	2.88417
8.0	2.86742	2.86716	2.86689	2.86660	2.86631	2.86600
9.0	2.85462	2.85434	2.85407	2.85378	2.85349	2.85320
10.0	2.84518	2.84492	2.84466	2.84440	2.84413	2.84386
15.0	2.82187	2.82172	2.82157	2.82142	2.82127	2.82112
20.0	2.81340	2.81331	2.81322	2.81313	2.81304	2.81294

Table 4.8. Frequency parameters for a simply supported super elliptical plate of [n=7]

a/b	$\lambda^2 = \omega(b^2 \sqrt{\rho h / D})$					
	v=0	v = 0.1	v = 0.2	v = 0.3	v= 0.4	v = 0.5
1.0	4.59176	4.75886	4.91335	5.05689	5.19085	5.31635
1.1	4.20845	4.35902	4.49823	4.62755	4.74823	4.86126
1.2	3.94143	4.07611	4.20065	4.31633	4.42424	4.52526
1.3	3.75150	3.87141	3.98230	4.08528	4.18129	4.27111
1.4	3.61368	3.72012	3.81854	3.90992	3.99507	4.07465
1.5	3.51167	3.60597	3.69316	3.77407	3.84940	3.91974
1.6	3.43465	3.51810	3.59524	3.66678	3.73332	3.79538
1.7	3.37532	3.44911	3.51729	3.58047	3.63919	3.69387
1.8	3.32865	3.39386	3.45408	3.50985	3.56162	3.60977
1.9	3.29115	3.34876	3.40193	3.45112	3.49673	3.53910
2.0	3.26038	3.31125	3.35817	3.40154	3.44171	3.47898
2.5	3.16056	3.18773	3.21271	3.23571	3.25690	3.27643
3.0	3.09847	3.11290	3.12614	3.13828	3.14942	3.15962
3.5	3.05086	3.05851	3.06551	3.07189	3.07772	3.08302
4.0	3.01232	3.01636	3.02002	3.02334	3.02634	3.02904
4.5	2.98094	2.98302	2.98488	2.98655	2.98802	2.98932
5.0	2.95540	2.95641	2.95729	2.95804	2.95868	2.95921
6.0	2.91759	2.91766	2.91769	2.91765	2.91758	2.91745
7.0	2.89200	2.89178	2.89154	2.89127	2.89098	2.89066
8.0	2.87418	2.87388	2.87357	2.87324	2.87290	2.87255
9.0	2.86139	2.86108	2.86077	2.86044	2.86011	2.85978
10.0	2.85195	2.85166	2.85136	2.85107	2.85076	2.85046
15.0	2.82859	2.82842	2.82825	2.82808	2.82791	2.82774
20.0	2.82008	2.81998	2.81988	2.81977	2.81967	2.81957

Table 4.9. Frequency parameters for a simply supported super elliptical plate of [n=8]

a/b	$\lambda^2 = \omega(b^2 \sqrt{\rho h / D})$					
	v=0	v = 0.1	v = 0.2	v = 0.3	v= 0.4	v = 0.5
1.0	4.59193	4.75912	4.91372	5.05740	5.19152	5.31721
1.1	4.20865	4.35931	4.49862	4.62808	4.74890	4.86211
1.2	3.94157	4.07637	4.20103	4.31687	4.42494	4.52614
1.3	3.75156	3.87162	3.98267	4.08583	4.18203	4.27205
1.4	3.61366	3.72030	3.81893	3.91052	3.99587	4.07567
1.5	3.51160	3.60614	3.69357	3.77473	3.85030	3.92086
1.6	3.43456	3.51829	3.59571	3.66752	3.73432	3.79662
1.7	3.37525	3.44935	3.51784	3.58132	3.64031	3.69526
1.8	3.32864	3.39420	3.45475	3.51083	3.56289	3.61130
1.9	3.29125	3.34922	3.40273	3.45225	3.49816	3.54080
2.0	3.26061	3.31186	3.35913	3.40283	3.44330	3.48084
2.5	3.16179	3.18932	3.21464	3.23794	3.25939	3.27914
3.0	3.10085	3.11556	3.12904	3.14140	3.15272	3.16307
3.5	3.05420	3.06204	3.06919	3.07571	3.08164	3.08702
4.0	3.01637	3.02051	3.02426	3.02766	3.03071	3.03344
4.5	2.98546	2.98760	2.98951	2.99120	2.99269	2.99399
5.0	2.96024	2.96127	2.96216	2.96292	2.96356	2.96407
6.0	2.92277	2.92283	2.92284	2.92279	2.92268	2.92253
7.0	2.89733	2.89709	2.89682	2.89652	2.89620	2.89585
8.0	2.87957	2.87924	2.87890	2.87855	2.87818	2.87780
9.0	2.86680	2.86647	2.86613	2.86578	2.86542	2.86506
10.0	2.85736	2.85705	2.85673	2.85641	2.85609	2.85576
15.0	2.83398	2.83380	2.83362	2.83343	2.83325	2.83307
20.0	2.82545	2.82534	2.82523	2.82512	2.82501	2.82490

Table 4.10. Frequency parameters for a simply supported super elliptical plate of [n=9]

a/b	$\lambda^2 = \omega(b^2 \sqrt{\rho h / D})$					
	v=0	v = 0.1	v = 0.2	v = 0.3	v= 0.4	v = 0.5
1.0	4.59176	4.75904	4.91375	5.05756	5.19184	5.31771
1.1	4.20852	4.35926	4.49868	4.62827	4.74924	4.86261
1.2	3.94141	4.07632	4.20111	4.31708	4.42531	4.52668
1.3	3.75134	3.87155	3.98275	4.08608	4.18245	4.27265
1.4	3.61339	3.72021	3.81902	3.91080	3.99635	4.07634
1.5	3.51129	3.60605	3.69370	3.77506	3.85085	3.92162
1.6	3.43425	3.51823	3.59588	3.66793	3.73496	3.79749
1.7	3.37495	3.44934	3.51809	3.58183	3.64106	3.69624
1.8	3.32840	3.39426	3.45510	3.51145	3.56376	3.61242
1.9	3.29109	3.34938	3.40320	3.45299	3.49916	3.54205
2.0	3.26057	3.31214	3.35973	3.40371	3.44445	3.48222
2.5	3.16258	3.19044	3.21605	3.23961	3.26129	3.28125
3.0	3.10261	3.11757	3.13127	3.14382	3.15530	3.16580
3.5	3.05678	3.06478	3.07208	3.07873	3.08476	3.09023
4.0	3.01956	3.02380	3.02764	3.03111	3.03421	3.03699
4.5	2.98906	2.99126	2.99321	2.99495	2.99646	2.99778
5.0	2.96412	2.96518	2.96609	2.96687	2.96751	2.96802
6.0	2.92696	2.92702	2.92702	2.92696	2.92685	2.92668
7.0	2.90166	2.90140	2.90112	2.90080	2.90046	2.90010
8.0	2.88395	2.88361	2.88326	2.88288	2.88250	2.88209
9.0	2.87121	2.87086	2.87051	2.87014	2.86977	2.86938
10.0	2.86178	2.86146	2.86112	2.86079	2.86045	2.86010
15.0	2.83839	2.83820	2.83801	2.83782	2.83763	2.83744
20.0	2.82985	2.82974	2.82962	2.82951	2.82939	2.82927

Table 4.11. Frequency parameters for a simply supported super elliptical plate of [n=10]

a/b	$\lambda^2 = \omega(b^2 \sqrt{\rho h / D})$					
	v=0	v = 0.1	v = 0.2	v = 0.3	v= 0.4	v = 0.5
1.0	4.59141	4.75878	4.91360	5.05754	5.19195	5.31798
1.1	4.20822	4.35905	4.49857	4.62828	4.74938	4.86290
1.2	3.94109	4.07611	4.20101	4.31712	4.42548	4.52700
1.3	3.75099	3.87133	3.98267	4.08614	4.18267	4.27302
1.4	3.61300	3.71997	3.81895	3.91090	3.99662	4.07678
1.5	3.51087	3.60582	3.69366	3.77521	3.85118	3.92215
1.6	3.43382	3.51802	3.59589	3.66814	3.73538	3.79811
1.7	3.37455	3.44918	3.51816	3.58212	3.64157	3.69696
1.8	3.32805	3.39416	3.45525	3.51184	3.56437	3.61324
1.9	3.29081	3.34937	3.40345	3.45349	3.49989	3.54299
2.0	3.26038	3.31224	3.36009	3.40433	3.44530	3.48329
2.5	3.16310	3.19124	3.21710	3.24089	3.26278	3.28292
3.0	3.10395	3.11913	3.13303	3.14575	3.15739	3.16801
3.5	3.05883	3.06698	3.07441	3.08117	3.08731	3.09286
4.0	3.02213	3.02647	3.03039	3.03393	3.03709	3.03992
4.5	2.99200	2.99425	2.99626	2.99803	2.99957	3.00091
5.0	2.96731	2.96840	2.96933	2.97013	2.97078	2.97130
6.0	2.93042	2.93049	2.93049	2.93043	2.93030	2.93012
7.0	2.90524	2.90498	2.90469	2.90436	2.90401	2.90363
8.0	2.88760	2.88724	2.88688	2.88649	2.88609	2.88568
9.0	2.87488	2.87452	2.87415	2.87378	2.87339	2.87299
10.0	2.86546	2.86513	2.86479	2.86444	2.86408	2.86373
15.0	2.84208	2.84188	2.84169	2.84149	2.84129	2.84109
20.0	2.83353	2.83341	2.83329	2.83317	2.83305	2.83293

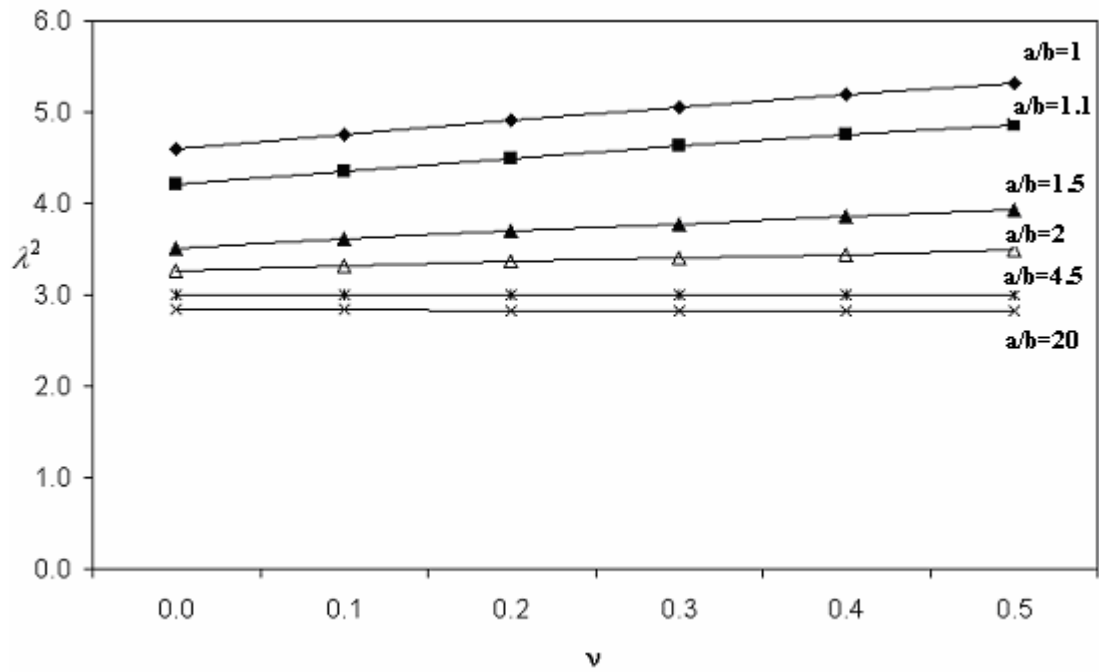


Fig. 4.2, Change of the frequency parameter λ^2 of a simply supported super elliptical plate of $n=1$ with respect to ν .

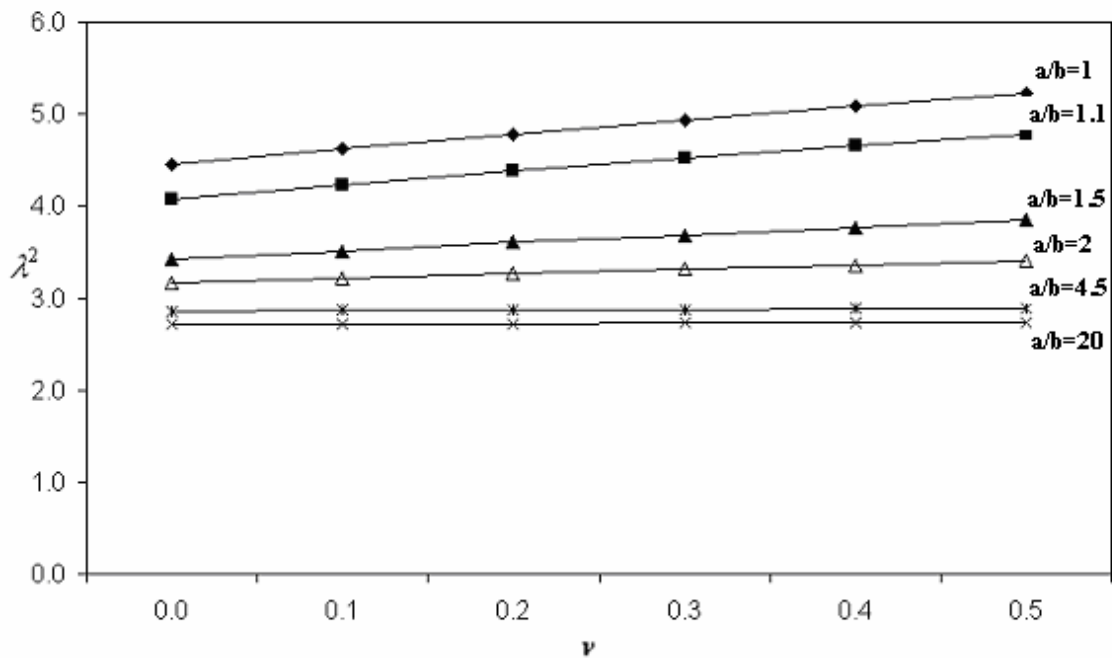


Fig. 4.3, Change of the frequency parameter λ^2 of a simply supported super elliptical plate of $n=10$ with respect to ν .

5. STATIC ANALYSES OF FUNCTIONALLY GRADED SUPER ELLIPTICAL PLATES

Elastic, functionally graded material (FGM) Kirchhoff plates have been investigated. For static analysis, uniformly distributed surface load and clamped boundary is assumed. Galerkin's method is used to solve the partial differential equation of plates. The Poisson's ratios of the plates are assumed to be constant, but their Young's moduli vary in the thickness direction functionally. Super elliptical plates include a wide range of geometrical shapes varying from a circle to a rectangle. The objective here is to investigate the influence of volume fractions and the component materials on static behavior of this class of plates.

This work is motivated by the increased demand to the FGM and the need to understand the behavior of FGM members. The study is conducted for a wide range of super elliptical plates. This study examines the static behavior of super elliptical plates considering sensitivities to different super ellipticity degrees. The results are also examined with respect to the parameters a/b ratios and n which are the plate aspect ratio and the super elliptical power, respectively. The demand of material properties can be satisfied by organizing the material composition by the power law exponent. Therefore the numerical work is conducted for various exponents.

5.1. Material Properties

The functionally graded plates are assumed to be mixture of ceramic and metal. The top surface material is ceramic (zirconia) rich and bottom surface material is metal (aluminum) rich. The material properties change in the thickness direction. For the validity of classical thin plate theory the transverse deflections are assumed to be small compared to the plate thickness.

FGM plates are composed of more than one material. Therefore, the effective material properties of the mixture govern the plate behavior. The composition of the material is assumed to be governed by a simple volume fraction rule. The volume fraction can be expressed as a power law function:

$$V(z) = \left(\frac{z + h/2}{h} \right)^N \quad (5.1)$$

where N is the power law exponent ($0 \leq N \leq \infty$), h the plate thickness, and z the coordinate in the thickness direction. The Young's modulus, Poisson's ratio, and density of the plate material vary continuously according to the volume fraction rule, Eq. (5.1). The variations of the volume fractions, which represent the variation of the mechanical properties of constituent materials, are illustrated in Fig. 5.1. It is seen that for high N values the effective material properties first exhibit changes in small increments and then rapidly change at the opposite side. For the low values of N the material properties change quickly near the surface.

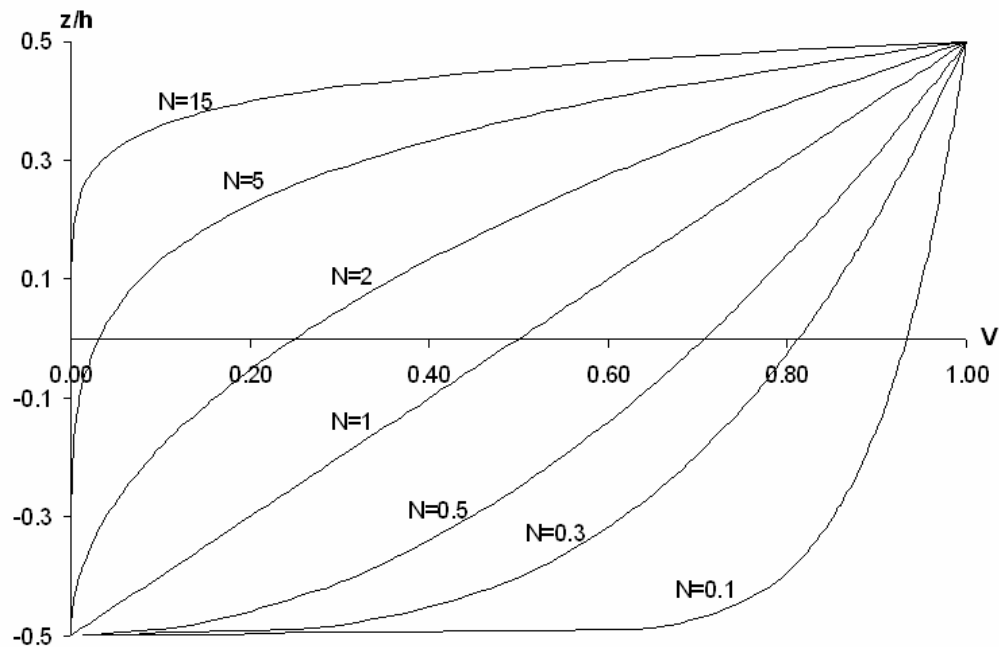


Fig.5.1. Through-the-thickness distribution of the volume fraction of the ceramic.

The volume fraction of metal may be derived from volume fraction of ceramic as:

$$V_{metal} = 1 - V_{ceramic} \quad (5.2)$$

Any effective material property, P_{eff} , of the dual material plate can be expressed as:

$$P_{eff} = P_{top}V_{top} + P_{bot}V_{bot} \quad (5.3)$$

where P_{top} and P_{bot} are the material properties of the top surface and bottom surface materials, respectively. V_{top} and V_{bot} are the volume fractions of the same materials, respectively. From Eqs. (5.1) and (5.3) the effective Young's modulus, E_{eff} , and effective mass density, $\bar{\rho}_{eff}$, are derived as:

$$E_{eff}(z) = E_{top}V(z) + E_{bot}(1 - V(z)) \quad (5.4)$$

$$\bar{\rho}_{eff}(z) = \bar{\rho}_{top}V(z) + \bar{\rho}_{bot}(1 - V(z)) \quad (5.5)$$

It should be noted that the effective properties obtained by using Eqs. (5.4) and (5.5) are position dependent in the thickness (z) direction. The position independent effective mass per unit area, ρ_{eff} , of the plate can be obtained by integrating over the thickness as:

$$\rho_{eff} = \int_{-h/2}^{h/2} \bar{\rho}_{eff}(z) dz \quad (5.6)$$

where h is the plate thickness. In the same way the effective bending rigidity, D_{eff} , of the plate can be obtained as

$$D_{eff} = \int_{-h/2}^{h/2} \frac{E_{eff}(z)}{1 - \nu_{eff}^2(z)} z^2 dz \quad (5.7)$$

where ν_{eff} is the effective Poisson's ratio of the FGM plate. Delale and Erdogan [45] indicated that the effect of Poisson's ratio on the deformation is negligible, but the effect of Young's modulus is highly effective. Thus, Poisson's ratio is assumed to be constant and Young's modulus is assumed to vary in the thickness direction.

For numerical calculations the following properties are used for the ceramic and metal materials:

$$E_c = 200 \text{ GPa}$$

$$E_m = 70 \text{ Gpa}$$

$$\rho_c = 5700 \text{ kg/m}^3$$

$$\rho_m = 2702 \text{ kg/m}^3$$

$$\nu_c = 0.3$$

$$\nu_m = 0.3$$

5.2. Basic Equations and Assumptions

The geometrical shapes of the studied plates are super elliptical. In order to deal with the plate bending problem a complete set of independent, continuous functions which are capable of representing the plate deflection are selected, as follows:

$$w(x, y) = \alpha_{ij} f_{ij}(x, y) = \sum_{i=1}^k \sum_{j=1}^k \alpha_{ij} \left(\frac{x^{2n}}{a^{2n}} + \frac{y^{2n}}{b^{2n}} \right)^2 x^i y^j, \quad i+j \leq k \quad (5.8)$$

Each term of this expression must satisfy all boundary conditions of the problem. In the static analysis, shape functions at the length of $k=8$ are used. Knowing that the displacement function of the studied loading and boundary conditions is an even function the odd powered terms are removed from the function. Since the governing differential equation of plates subjected to lateral load q_0 is based on the equilibrium of the internal and external forces in the

z direction, the total work, performed by all these forces, during a small virtual δw displacement can be expressed by

$$\iint_A (\nabla^4 w - \frac{q_0}{D_{eff}}) \delta w dx dy = 0 \quad (5.9)$$

This equation represents the basic variational equation of plate bending. Substituting this expression into Eq. (5.8) gives:

$$\sum_{i=1}^n \delta c_i \iint_A [\nabla^4 w(x, y) - \frac{q_0}{D_{eff}}] \alpha_{ij} f_{ij}(x, y) dx dy = 0 \quad (5.10)$$

Eq. (5.10) must be satisfied for any values of δc_i , and it follows that

$$\begin{aligned} \iint_A (\nabla^4 w - \frac{q_0}{D_{eff}}) \alpha_{00} f_{00}(x, y) dx dy &= 0 \\ \iint_A (\nabla^4 w - \frac{q_0}{D_{eff}}) \alpha_{02} f_{02}(x, y) dx dy &= 0 \\ \dots\dots\dots \\ \iint_A (\nabla^4 w - \frac{q_0}{D_{eff}}) \alpha_{0k} f_{0k}(x, y) dx dy &= 0 \end{aligned} \quad (5.11)$$

The integrals are evaluated over the entire surface of the plate. In this way the solution of the differential equation of the plate is reduced to the evaluation of definite integrals of simple functions. After the evaluation of the integrals a set of linear equations is obtained. The number of equations is equal to the number of unknown coefficients α_{ij} in Eq. (5.8), and then the displacement function is obtained.

5.3. Results of Static Analyses

The maximum deflections of the FGM super elliptical plates under static loading are obtained and parameterized as $\Delta = w_{max}(h^3/q_0)(10^9)$. During the static analysis one dimension of the super ellipses is kept constant ($b=1$). The results for 3 super elliptical forms and for a wide range of a/b ratios are presented in Figs. 5.2-5.4 For purpose of comparison, the study is also conducted for a homogeneous material plate in terms of the parameter $\lambda = w_{max}(D/q_0)$, where D is the flexural rigidity of the plate. The geometrical shape of the super ellipse with $n=10$ is very similar to a rectangle. In Table 5.1. the λ value obtained for $a=1$ and $b=1$ is compared with the corresponding square.

Table 5.1. Comparison of the displacement parameter ($\lambda = w_{max}(D/q_0)$,) with previously obtained results

n=10	Rectangle	
	Timoshenko [11]	Shames[7]
0.02017	0.0202	0.02067

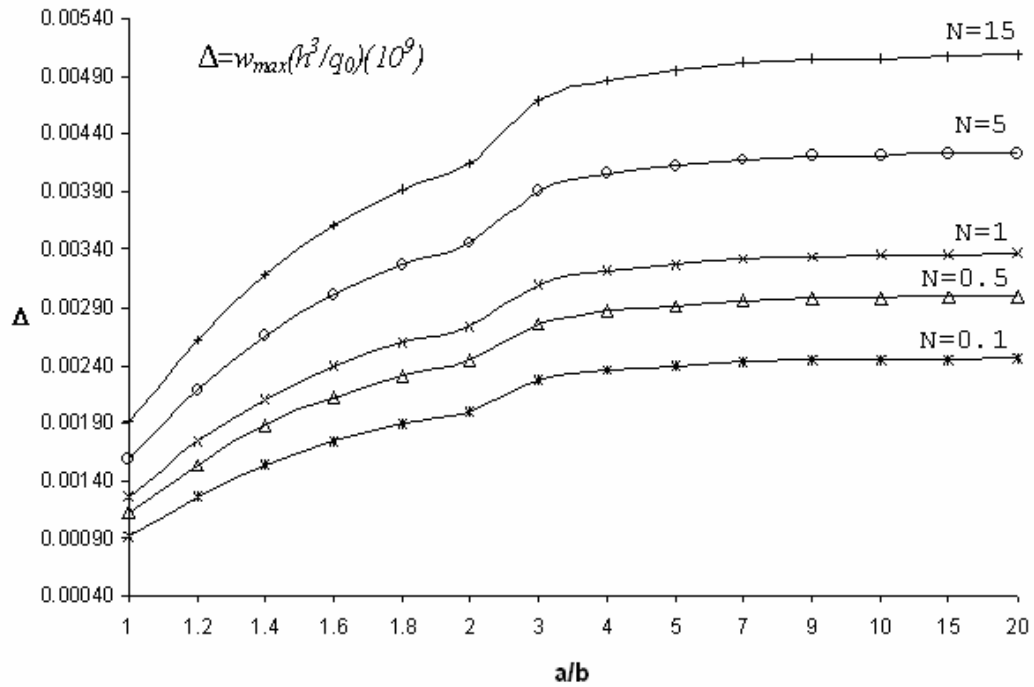


Fig.5.2 Maximum static deflections of the super elliptical plates of $n=1$ (elliptical)

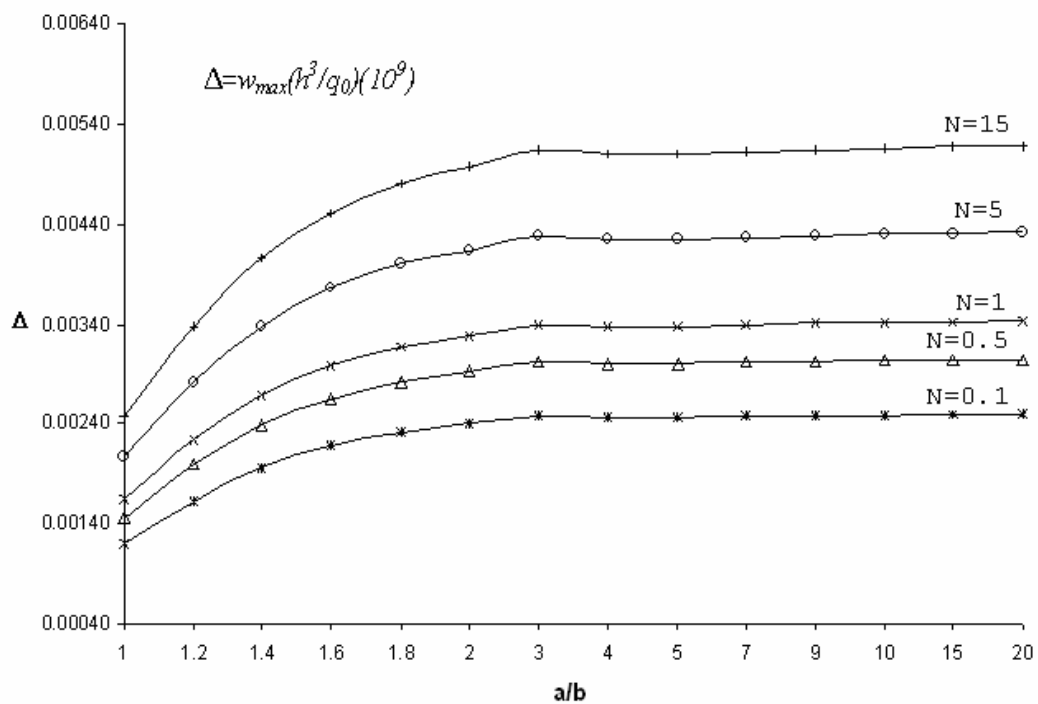


Fig.5.3 Maximum static deflections of the super elliptical plates of $n=4$

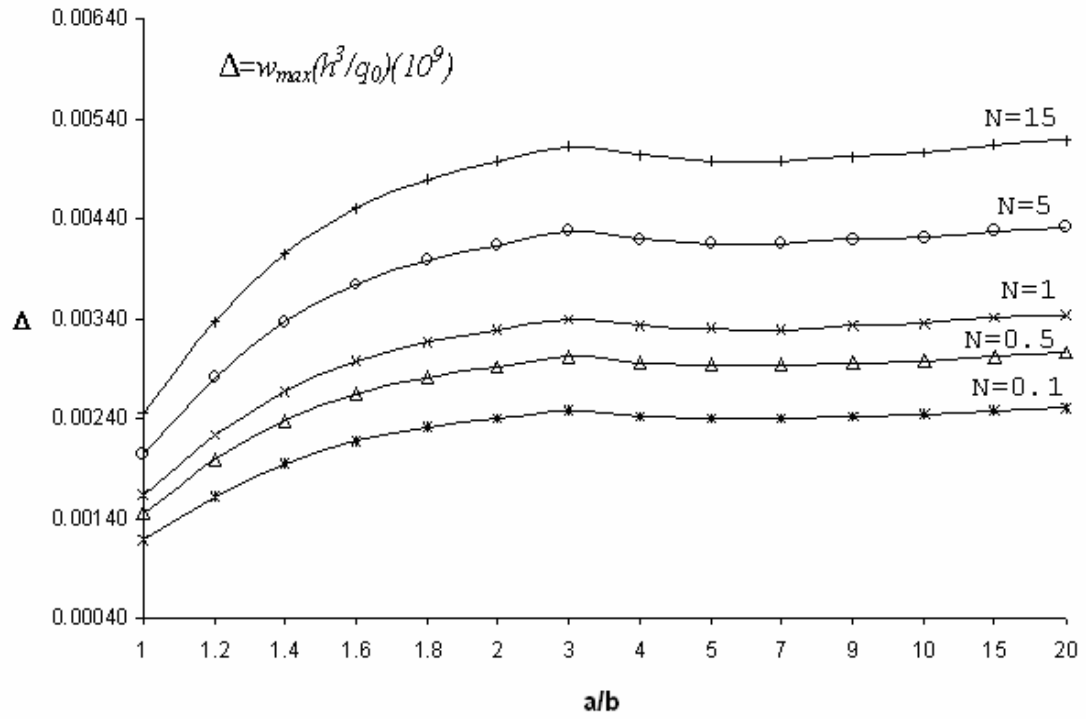


Fig.5.4 Maximum static deflections of the super elliptical plates of $n=10$

6. FREE VIBRATION OF SIMPLY SUPPORTED FGM SUPER ELLIPTICAL PLATES

In addition to static analyses, free vibration characteristics of simply supported FGM plates are studied by using Ritz method.

This study examines the static behavior and free vibration of super elliptical plates considering sensitivities of the frequency parameters to different super ellipticity degrees. The results are also examined with respect to the parameters a/b ratios and n which are the plate aspect ratio and the super elliptical power, respectively.

6.1. Basic Equations and Assumptions

The expression for the strain energy of the plate is:

$$U = \frac{1}{2} \iint_A D_{eff} \left\{ \left(\frac{\partial^2 w}{\partial x^2} + \frac{\partial^2 w}{\partial y^2} \right)^2 - 2(1 - \nu_{eff}) \left[\frac{\partial^2 w}{\partial x^2} \frac{\partial^2 w}{\partial y^2} - \left(\frac{\partial^2 w}{\partial x \partial y} \right)^2 \right] \right\} dx dy \quad (6.1)$$

The expression representing the kinetic energy of the plate is:

$$T = \frac{1}{2} \iint_A \rho_{eff} h(x, y) \left[\frac{\partial w(x, y, t)}{\partial t} \right]^2 dx dy \quad (6.2)$$

In order to apply Ritz method firstly an appropriate deflection shape, Eq. (6.4), is selected and then maximum kinetic and strain energies are equated. An equation in the following form is obtained:

$$E = \frac{1}{2} \iint_A D_{eff} \left\{ \left(\frac{\partial^2 w}{\partial x^2} + \frac{\partial^2 w}{\partial y^2} \right)^2 - 2(1 - \nu_{eff}) \left[\frac{\partial^2 w}{\partial x^2} \frac{\partial^2 w}{\partial y^2} - \left(\frac{\partial^2 w}{\partial x \partial y} \right)^2 \right] \right\} dx dy -$$

$$\frac{\omega^2}{2} \iint_A \rho_{eff} h(x, y) w^2(x, y) dx dy = 0 \quad (6.3)$$

For the dynamic analyses a trial function for deflection of middle surface, w , may be represented by

$$w = \left(\frac{x^{2n}}{a^{2n}} + \frac{y^{2n}}{b^{2n}} - 1 \right) \left(\alpha_{00} + \alpha_{20} \frac{x^2}{a^2} + \alpha_{02} \frac{y^2}{b^2} \right) \quad (6.4)$$

where α_{00} , α_{20} , and α_{02} are the unknown coefficients. The chosen deflection function possesses such a property that it has the form of two-fold symmetry which is required for the fundamental vibration mode. Eq. (6.3) is minimized with respect to unknown coefficients, α_{00} , α_{20} , and α_{02} . This procedure yields a set of homogeneous linear equations in terms of α_{ij} and in this way the problem is reduced to an eigenvalue problem.

The unknown constants α_{00} , α_{20} , and α_{02} are determined from the minimum potential energy principle as:

$$\frac{\partial E}{\partial \alpha_{00}} = 0, \quad \frac{\partial E}{\partial \alpha_{20}} = 0 \quad \text{and} \quad \frac{\partial E}{\partial \alpha_{02}} = 0 \quad (6.5)$$

With this minimization procedure, three simultaneous algebraic equations, in terms of the unknown coefficients α_{00} , α_{20} , and α_{02} , will be obtained. The number of equations is equal to the number of the unknown parameters, so α_{00} , α_{20} , and α_{02} can be calculated.

6.2. Results of the Free Vibration Analyses

The results of the dynamic analysis pertinent to the selected shape function are presented in Tables 6.1-6.7. In order to investigate the effect of volume fractions, the results are also obtained for homogeneous constituent materials, ceramic and metal.

Table 6.1. Frequency parameters, $10^4 \omega b^2/h$, for simply supported super elliptical plates made of ceramic

a/b	n						
	1	2	3	4	6	8	10
1.0	3.62691	3.68090	3.69877	3.70625	3.71145	3.71267	3.71277
1.2	3.09632	3.14113	3.15651	3.16309	3.16784	3.16904	3.16922
1.4	2.80472	2.84454	2.85866	2.86485	2.86946	2.87073	2.87101
1.6	2.62902	2.66620	2.67985	2.68602	2.69085	2.69234	2.69280
1.8	2.51404	2.54994	2.56366	2.57010	2.57544	2.57732	2.57806
2.0	2.43316	2.46857	2.48269	2.48958	2.49565	2.49804	2.49914
3.0	2.22820	2.26377	2.28077	2.29044	2.30079	2.30612	2.30932
4.0	2.13874	2.17297	2.19124	2.20244	2.21539	2.22262	2.22722
5.0	2.09087	2.12288	2.14122	2.15293	2.16698	2.17510	2.18039
7.0	2.04525	2.07361	2.09130	2.10306	2.11766	2.12635	2.13211
9.0	2.02545	2.05164	2.06874	2.08035	2.09498	2.10378	2.10965
15.0	2.00553	2.02911	2.04542	2.05674	2.07122	2.08004	2.08595
20.0	2.00057	2.02342	2.03949	2.05071	2.06513	2.07394	2.07985

Table 6.2. Frequency parameters, $10^4 \omega b^2/h$, for simply supported super elliptical plates which have material composition of $N=0.1$

a/b	n						
	1	2	3	4	6	8	10
1.0	3.43650	3.48765	3.50459	3.51167	3.51660	3.51775	3.51785
1.2	2.93376	2.97622	2.99079	2.99703	3.00153	3.00266	3.00284
1.4	2.65748	2.69521	2.70858	2.71445	2.71881	2.72002	2.72028
1.6	2.49100	2.52622	2.53916	2.54501	2.54958	2.55100	2.55143
1.8	2.38205	2.41607	2.42907	2.43517	2.44023	2.44201	2.44271
2.0	2.30542	2.33897	2.35235	2.35888	2.36463	2.36689	2.36793
3.0	2.11122	2.14492	2.16103	2.17020	2.18000	2.18505	2.18808
4.0	2.02646	2.05889	2.07620	2.08681	2.09908	2.10593	2.11029
5.0	1.98110	2.01143	2.02881	2.03990	2.05321	2.06091	2.06592
7.0	1.93788	1.96475	1.98150	1.99265	2.00649	2.01472	2.02018
9.0	1.91911	1.94393	1.96013	1.97113	1.98499	1.99334	1.99890
15.0	1.90024	1.92258	1.93803	1.94876	1.96248	1.97084	1.97644
20.0	1.89554	1.91719	1.93241	1.94305	1.95671	1.96505	1.97066

Table 6.3. Frequency parameters, $10^4 \omega b^2/h$, for simply supported super elliptical plates which have material composition of $N=0.5$

a/b	n						
	1	2	3	4	6	8	10
1.0	3.02964	3.07474	3.08967	3.09591	3.10026	3.10127	3.10136
1.2	2.58642	2.62386	2.63670	2.64220	2.64616	2.64717	2.64732
1.4	2.34285	2.37611	2.38790	2.39307	2.39692	2.39799	2.39822
1.6	2.19608	2.22714	2.23854	2.24369	2.24773	2.24898	2.24936
1.8	2.10003	2.13002	2.14148	2.14686	2.15132	2.15289	2.15351
2.0	2.03247	2.06205	2.07384	2.07960	2.08467	2.08667	2.08759
3.0	1.86126	1.89098	1.90518	1.91326	1.92190	1.92635	1.92902
4.0	1.78654	1.81513	1.83039	1.83975	1.85056	1.85660	1.86045
5.0	1.74655	1.77329	1.78861	1.79839	1.81012	1.81691	1.82133
7.0	1.70844	1.73214	1.74691	1.75674	1.76893	1.77619	1.78100
9.0	1.69190	1.71378	1.72807	1.73777	1.74998	1.75734	1.76224
15.0	1.67527	1.69496	1.70858	1.71804	1.73014	1.73750	1.74244
20.0	1.67112	1.69021	1.70363	1.71301	1.72505	1.73241	1.73734

Table 6.4. Frequency parameters, $10^4 \omega b^2/h$, for simply supported super elliptical plates which have material composition of $N=1$

a/b	n						
	1	2	3	4	6	8	10
1.0	2.85169	2.89413	2.90819	2.91406	2.91816	2.91911	2.91919
1.2	2.43450	2.46974	2.48183	2.48701	2.49073	2.49168	2.49182
1.4	2.20523	2.23654	2.24764	2.25251	2.25613	2.25713	2.25735
1.6	2.06709	2.09632	2.10705	2.11191	2.11570	2.11688	2.11724
1.8	1.97668	2.00491	2.01570	2.02076	2.02496	2.02644	2.02702
2.0	1.91309	1.94093	1.95203	1.95745	1.96223	1.96410	1.96497
3.0	1.75194	1.77990	1.79327	1.80088	1.80902	1.81320	1.81572
4.0	1.68160	1.70851	1.72288	1.73169	1.74187	1.74755	1.75117
5.0	1.64396	1.66913	1.68355	1.69276	1.70380	1.71019	1.71435
7.0	1.60809	1.63039	1.64430	1.65355	1.66503	1.67186	1.67639
9.0	1.59252	1.61312	1.62656	1.63569	1.64719	1.65412	1.65873
15.0	1.57687	1.59540	1.60822	1.61712	1.62851	1.63545	1.64010
20.0	1.57296	1.59093	1.60356	1.61239	1.62373	1.63065	1.63530

Table 6.5. Frequency parameters, $10^4 \omega b^2/h$, for simply supported super elliptical plates which have material composition of $N=5$

a/b	n						
	1	2	3	4	6	8	10
1.0	2.59250	2.63109	2.64387	2.64921	2.65293	2.65380	2.65387
1.2	2.21324	2.24527	2.25626	2.26097	2.26436	2.26522	2.26535
1.4	2.00481	2.03327	2.04336	2.04778	2.05108	2.05199	2.05219
1.6	1.87921	1.90579	1.91555	1.91996	1.92341	1.92448	1.92481
1.8	1.79703	1.82269	1.83250	1.83710	1.84092	1.84226	1.84279
2.0	1.73922	1.76453	1.77462	1.77954	1.78388	1.78559	1.78637
3.0	1.59271	1.61813	1.63029	1.63720	1.64460	1.64841	1.65069
4.0	1.52877	1.55323	1.56629	1.57430	1.58355	1.58872	1.59201
5.0	1.49455	1.51743	1.53054	1.53891	1.54895	1.55475	1.55853
7.0	1.46194	1.48221	1.49485	1.50326	1.51370	1.51991	1.52403
9.0	1.44778	1.46650	1.47873	1.48703	1.49748	1.50378	1.50797
15.0	1.43355	1.45040	1.46206	1.47015	1.48050	1.48681	1.49103
20.0	1.43000	1.44633	1.45782	1.46584	1.47615	1.48244	1.48667

Table 6.6. Frequency parameters, $10^4 \omega b^2/h$, for simply supported super elliptical plates which have material composition of $N=15$

a/b	n						
	1	2	3	4	6	8	10
1.0	2.27395	2.30780	2.31901	2.32370	2.32696	2.32772	2.32778
1.2	1.94129	1.96938	1.97903	1.98316	1.98613	1.98688	1.98700
1.4	1.75847	1.78344	1.79228	1.79617	1.79906	1.79986	1.80003
1.6	1.64831	1.67162	1.68018	1.68405	1.68707	1.68801	1.68830
1.8	1.57622	1.59873	1.60733	1.61137	1.61472	1.61590	1.61636
2.0	1.52551	1.54771	1.55656	1.56089	1.56469	1.56619	1.56688
3.0	1.39701	1.41931	1.42997	1.43603	1.44252	1.44586	1.44787
4.0	1.34092	1.36238	1.37384	1.38086	1.38898	1.39351	1.39640
5.0	1.31091	1.33098	1.34248	1.34982	1.35862	1.36371	1.36703
7.0	1.28230	1.30009	1.31117	1.31855	1.32771	1.33315	1.33676
9.0	1.26989	1.28631	1.29703	1.30431	1.31348	1.31900	1.32268
15.0	1.25740	1.27219	1.28241	1.28951	1.29859	1.30412	1.30782
20.0	1.25429	1.26862	1.27869	1.28573	1.29477	1.30029	1.30400

Table 6.7. Frequency parameters, $10^4 \omega b^2/h$, for simply supported super elliptical plates made of metal

a/b	n						
	1	2	3	4	6	8	10
1.0	1.84374	1.87118	1.88027	1.88407	1.88672	1.88733	1.88738
1.2	1.57401	1.59679	1.60461	1.60796	1.61037	1.61098	1.61107
1.4	1.42578	1.44602	1.45320	1.45635	1.45869	1.45934	1.45948
1.6	1.33646	1.35536	1.36230	1.36544	1.36789	1.36865	1.36889
1.8	1.27801	1.29626	1.30324	1.30651	1.30922	1.31018	1.31056
2.0	1.23690	1.25490	1.26207	1.26558	1.26866	1.26988	1.27044
3.0	1.13270	1.15079	1.15943	1.16435	1.16961	1.17232	1.17394
4.0	1.08723	1.10463	1.11392	1.11961	1.12619	1.12987	1.13221
5.0	1.06289	1.07917	1.08849	1.09444	1.10158	1.10571	1.10840
7.0	1.03970	1.05412	1.06311	1.06909	1.07651	1.08093	1.08386
9.0	1.02964	1.04295	1.05164	1.05755	1.06498	1.06946	1.07244
15.0	1.01951	1.03150	1.03979	1.04554	1.05291	1.05739	1.06039
20.0	1.01699	1.02860	1.03677	1.04248	1.04981	1.05429	1.05729

7. CONCLUSIONS AND RECOMMENDATIONS

In this thesis static and dynamic analyses of super elliptical plates are studied with Kirchhoff plate model. Galerkin and Ritz approximation models are presented. The models are also employed for FGM plates. Some concluding remarks are as follows:

- Static behavior of super elliptical plates for various aspect ratios and integer powers which represent the geometrical shapes between an ellipse and a rectangle has been presented and good agreement is obtained between the rectangle and the super ellipse of $n=10$.
- Although the shapes are bounded with these boundaries a linear interpolation between these shapes does not necessarily give correct deflection parameters.
- In Chapter 3. the column of $n=10$ of the Tables 3.2-3.5 contain results for the shape nearest to a rectangle. The parameter value 0.02017 in Table 3.5. is in good agreement with the values presented in references [7] and [11] which are 0.02067 and 0.0202 respectively. The values obtained for ellipses including circle are exact and agree with the result of Shames [7] which is obtained by Ritz method.
- In Table 3.6 the results obtained for moments at the mid point of the plates are in good agreement with the reference [11].
- The influence of rounded corners on bending moment is studied. It is observed that rounding the corners decreases the flexural moments. For instance, the moment parameter for the super ellipse of $n=10$, nearest to the rectangle, is 19.3 % higher than that of the super ellipse of $n=4$, with relatively rounded corners.

- During the dynamic analysis the dependency of ν is observed for both high and low values of super elliptical powers, n . The ratio of λ^2 for $\nu=0$ and $\nu=0.5$ for $a/b=1$ in Table 4.2 which represents the results for an elliptical boundary shape ($n=1$) is 0.8521. The same ratio for $n=5$ and $n=10$ is 0.8638 and 0.8634 respectively. There is 14-15 % ν dependency.
- The dependency of the frequency parameters is also inspected for changing a/b values. The above indicated ratio of λ^2 for $n=1$, is determined as 0.9910 for $a/b=5$ and 0.9993 for $a/b=20$, which means that the Poisson's ratio dependency becomes very minimal for high aspect ratios of the super ellipses.
- The above indicated trend is valid for all super elliptical shapes examined in the current study.
- Static and dynamic analyses are also employed for FGM plates. The effect of volume fractions, aspect ratios, and super ellipticity power are worked in detail. From numerical results it is seen that the mechanical behavior characteristics of FGM plates remain between the characteristics of the constituent materials.
- The presented solution methods and results herein should be useful for engineers when considering this sort of plates with similar boundary conditions.

For future studies the following recommendations are introduced:

- The study may be conducted for plates of variable thickness.
- The effects of functional loadings and elastic boundary conditions may be studied.
- FGM plates are generally used in high temperature; therefore a study on thermal behavior of these plates should be useful.

APPENDIX : FREE VIBRATION EXAMPLE PREPARED BY USING MATHEMATICA 5.2

```
(***** Content-type: application/mathematica *****)
CreatedBy='Mathematica 5.2'
```

Mathematica-Compatible Notebook

This notebook can be used with any Mathematica-compatible application, such as Mathematica, MathReader or Publicon. The data for the notebook starts with the line containing stars above.

To get the notebook into a Mathematica-compatible application, do one of the following:

- * Save the data starting with the line of stars above into a file with a name ending in .nb, then open the file inside the application;
- * Copy the data starting with the line of stars above to the clipboard, then use the Paste menu command inside the application.

Data for notebooks contains only printable 7-bit ASCII and can be sent directly in email or through ftp in text mode. Newlines can be CR, LF or CRLF (Unix, Macintosh or MS-DOS style).

NOTE: If you modify the data for this notebook not in a Mathematica-compatible application, you must delete the line below containing the word CacheID, otherwise Mathematica-compatible applications may try to use invalid cache data.

For more information on notebooks and Mathematica-compatible applications, contact Wolfram Research:

web: <http://www.wolfram.com>

email: info@wolfram.com

phone: +1-217-398-0700 (U.S.)

Notebook reader applications are available free of charge from Wolfram Research.

*****)

(*CacheID: 232*)

```
(*NotebookFileLineBreakTest
NotebookFileLineBreakTest*)
(*NotebookOptionsPosition[ 30227, 612]*)
(*NotebookOutlinePosition[ 30872, 634]*)
(* CellTagsIndexPosition[ 30828, 630]*)
(*WindowFrame->Normal*)
```

```

Notebook[ {
Cell[BoxData[{\(a = 1;\), "[IndentingNewLine]", \(\n =
  10;\), "[IndentingNewLine]",
  RowBox[{\(\[Nu] = 0.4\), "[IndentingNewLine]", "[IndentingNewLine]",
  StyleBox[{\( (*\
    Vibration\ of\ superelliptical\ simply\ supported\ \((\
\([CapitalOmega] = 1)\) plates - Ritz*) \),
  FontColor->RGBColor[1, 0, 0]]}, "[IndentingNewLine]",
  RowBox[ {
    " ", \(\ll LinearAlgebra`MatrixManipulation`\);}, "[IndentingNewLine]",

  RowBox[{\(\ll Calculus`VectorAnalysis`\),
    "[IndentingNewLine"]}, "[IndentingNewLine]", \(\r =
    4.5\), "[IndentingNewLine]",
  RowBox[{\(b = a\sqrt{r}\),
    "[IndentingNewLine"]}, "[IndentingNewLine]", \(\d =
    1;\), "[IndentingNewLine]", \(\omega = \sqrt{(x^{2n})/a^{2n} + \
y^{2n}/b^{2n} - 1)}^{1/2}*(a^2 + a^2*y^2/b^2 +
    a^2*x^2/a^2)\), "[IndentingNewLine]",
  RowBox[{\(intbound = b*\sqrt{(1 - (x/a))^{2n})}\),
    "[IndentingNewLine"]}, "[IndentingNewLine]", \(\uU =
    \sqrt{2}*\integrate[\sqrt{(D[w, {x, 2}] + D[w, {y, 2}])^2 +
    2*\sqrt{(1 - \[Nu])}*\sqrt{(D[D[w, y], x])^2 -
    D[w, {x, 2}]*D[w, {y, 2}])}\), {y, \(-intbound\),
    intbound}\), "[IndentingNewLine]", \(\uU =
    \integrate[uU, {x, \(-1\), 1}\];\), "[IndentingNewLine]",
  RowBox[ {
    StyleBox[{\( (* uU is the strain energy due to bending *) \),
    FontColor->RGBColor[1, 0, 0]], "[IndentingNewLine]",
    StyleBox[
      RowBox[{"(*", " ",
        RowBox[{"d", "="},
        RowBox[ {
          FractionBox[
            SuperscriptBox[
              StyleBox["Eh",
                FontColor->RGBColor[1, 0, 0]],
                "3"], \sqrt{(1 - \[Nu]^2)}\), " ", "is", " ", "the",
                " ", "flexural", " ", "rigidity", " ", "of", " ", "the", " ",
                "plate"}], " ", "*)"}],
        FontColor->RGBColor[1, 0, 0],
        0]]}, "[IndentingNewLine]", \(\tT = \sqrt{\Lambda}*\
\integrate[
    w^2, {y, \(-intbound\),
    intbound}\];\), "[IndentingNewLine]", \(\tT =
    \integrate[tT, {x, \(-1\), 1}\];\), "[IndentingNewLine]",
    StyleBox[{\( (* \sqrt{\Lambda} = 1/2*\sqrt{\rho}*h*\sqrt{\Omega}^2 \ * *) \),
    FontColor->RGBColor[1, 0, 0]], "[IndentingNewLine]",
    StyleBox[{\( (* \tT is the kinetic energy *) \),
    FontColor->RGBColor[1, 0, 0]], "[IndentingNewLine]", \(\Print[
    thisisF]), "[IndentingNewLine]", \(\tF =
    uU - tT;\), "[IndentingNewLine]",
    StyleBox[{\( (* tF is the total energy functional *) \),

```

```

FontColor->RGBColor[1, 0,
0]], "[IndentingNewLine]", \(\eq1 =
D[fF, a00];\), "[IndentingNewLine]", \(\eq2 =
D[fF, a02];\), "[IndentingNewLine]",
RowBox[{\(\eq3 = D[fF, a20];\),
"[IndentingNewLine"]}], "[IndentingNewLine]", \(\eqs =
LinearEquationsToMatrices[{\eq1 \[Equal] 0, eq2 \[Equal] 0,
eq3 \[Equal] 0}, {a00, a02,
a20}];\), "[IndentingNewLine]", \(\deteqs =
eqs[1];\), "[IndentingNewLine]", \(\Print[
theequation]), "[IndentingNewLine]", \(\polinomialeq =
Det[deteqs] \ (*\
the\ determinant\ of\ the\ equations\ *) ;\), "[IndentingNewLine]", \
\(\Print[rootsoftheequation]), "[IndentingNewLine]", \(\sol =
Solve[polinomialeq \[Equal]
0, \[Lambda];\), "[IndentingNewLine]", \(\Print[
r]), "[IndentingNewLine]", \(\trfrsolution =
N[sol^0.5*\@2*
b^2]), "[IndentingNewLine]", \(\TimeUsed[]), \
"[IndentingNewLine]",
RowBox[{"bitti", "[IndentingNewLine]"}], "[IndentingNewLine]", \(\r =
5.0), "[IndentingNewLine]",
RowBox[{\(b = a/r\),
"[IndentingNewLine]"}], "[IndentingNewLine]", \(\d =
1;\), "[IndentingNewLine]", \(\w = \((x^(2\ n)/a^(2\ n)) + \
y^(2\ n)/b^(2\ n) - 1)\)^1*\((a00 + a02*y^2/b^2 +
a20*x^2/a^2)\)), "[IndentingNewLine]",
RowBox[{\(\intbound = b*\@((1 - \((x/a)^(2\ n))\)),
"[IndentingNewLine]"}], "[IndentingNewLine]", \(\uU =
d^2*Integrate[\((D[w, {x, 2}] + D[w, {y, 2}])\)^2 +
2*\((1 - \[Nu])\)*\((D[D[w, y], x])\)^2 -
D[w, {x, 2}]*D[w, {y, 2}]\)), {y, \(-intbound\),
intbound}], "[IndentingNewLine]", \(\uU =
Integrate[uUt, {x, \(-1\), 1}];\), "[IndentingNewLine]",
RowBox[{\
StyleBox[\( (*\ uU\ is\ the\ strain\ energy\ due\ to\ bending\ *) \),
FontColor->RGBColor[1, 0, 0]], "[IndentingNewLine]",
StyleBox[
RowBox[{"*", ""},
RowBox[{"d", "="},
RowBox[{\
FractionBox[
SuperscriptBox[
StyleBox["Eh",
FontColor->RGBColor[1, 0, 0]],
"3"], \((1 - \[Nu]^2)\)), "", "is", "", "the",
"", "flexural", "", "rigidity", "", "of", "", "the", "",
"plate"}];}], "", "*"}],
FontColor->RGBColor[1, 0,
0]]}], "[IndentingNewLine]", \(\tTt = \[Lambda]*
Integrate[
w^2, {y, \(-intbound\),
intbound}];\), "[IndentingNewLine]", \(\tT =
Integrate[tTt, {x, \(-1\), 1}];\), "[IndentingNewLine]",
StyleBox[\( (*\ \[Lambda] = 1/2*\[Rho]*h*\[Omega]^2\ *) \),

```

```

FontColor->RGBColor[1, 0, 0]], "[IndentingNewLine]",
StyleBox[( (* \ tT is the kinetic energy *) ),
FontColor->RGBColor[1, 0, 0]], "[IndentingNewLine]", \(\Print[
thisisF]), "[IndentingNewLine]", \(\fF =
uU - tT;), "[IndentingNewLine]",
StyleBox[( (* fF is the total energy functional *) ),
FontColor->RGBColor[1, 0,
0]], "[IndentingNewLine]", \(\eq1 =
D[fF, a00];), "[IndentingNewLine]", \(\eq2 =
D[fF, a02];), "[IndentingNewLine]",
RowBox[{\(\eq3 = D[fF, a20];),
"[IndentingNewLine"]}, "[IndentingNewLine]", \(\eqs =
LinearEquationsToMatrices[{\eq1 \[Equal] 0, eq2 \[Equal] 0,
eq3 \[Equal] 0}, {a00, a02,
a20};), "[IndentingNewLine]", \(\deteqs =
eqs[{\[1]}];), "[IndentingNewLine]", \(\Print[
theequation]), "[IndentingNewLine]", \(\polinomialeq =
Det[deteqs] \ (*\
the determinant of the equations *) ;), "[IndentingNewLine]", \
\(\Print[rootsoftheequation]), "[IndentingNewLine]", \(\sol =
Solve[polinomialeq \[Equal]
0, \[Lambda];), "[IndentingNewLine]", \(\Print[
r]), "[IndentingNewLine]", \(\trfrsolution =
N[sol^0.5*@\@2*
b^2]), "[IndentingNewLine]", \(\TimeUsed[]), \
"[IndentingNewLine]",
RowBox[{"bitti", "[IndentingNewLine"]}, "[IndentingNewLine]", \(\r =
6.0), "[IndentingNewLine]",
RowBox[{\(b = a\sqrt{r}),
"[IndentingNewLine"]}, "[IndentingNewLine]", \(\d =
1;), "[IndentingNewLine]", \(\w = \((x^\(2\ n)/a^\(2\ n) + \
y^\(2\ n)/b^\(2\ n) - 1)\)^\(1*(a00 + a02*y^\(2\ n)/b^\(2\ n) +
a20*x^\(2\ n)/a^\(2\ n))), "[IndentingNewLine]",
RowBox[{\(\intbound = b*@\((1 - \((x/a)^\(2\ n))\)),
"[IndentingNewLine"]}, "[IndentingNewLine]", \(\uU =
d\sqrt{2}*Integrate[\((D[w, {x, 2}] + D[w, {y, 2}])^\(2\ n) +
2*\((1 - \[Nu])\)*\((D[D[w, y], x])^\(2\ n) -
D[w, {x, 2}]*D[w, {y, 2}])\)), {y, \(-intbound),
intbound};), "[IndentingNewLine]", \(\uU =
Integrate[uUt, {x, \(-1), 1};), "[IndentingNewLine]",
RowBox[{\
StyleBox[( (* uU is the strain energy due to bending *) ),
FontColor->RGBColor[1, 0, 0]], "[IndentingNewLine]",
StyleBox[
RowBox[{"(", " ",
RowBox[{"d", "="},
RowBox[{\
FractionBox[
SuperscriptBox[
StyleBox["Eh",
FontColor->RGBColor[1, 0, 0]],
"3"], \((1 - \[Nu]^\(2\ n))\)), " ", "is", " ", "the",
" ", "flexural", " ", "rigidity", " ", "of", " ", "the", " ",
"plate"}]}], " ", "*)"}],
FontColor->RGBColor[1, 0,

```

```

0]]}, "[IndentingNewLine]", \(\tT = \[\Lambda]*
  Integrate[
    w^2, {y, \(-intbound),
      intbound};\), "[IndentingNewLine]", \(\tT =
    Integrate[\tT, {x, \(-1), 1};\), "[IndentingNewLine]",
StyleBox[\( (* \[\Lambda] = 1/2*\[\Rho]*h*\[\Omega]^\w2 \ * ) \),
  FontColor->RGBColor[1, 0, 0]], "[IndentingNewLine]",
StyleBox[\( (* \ tT is the kinetic energy \ * ) \),
  FontColor->RGBColor[1, 0, 0]], "[IndentingNewLine]", \(\Print[
thisisfF]), "[IndentingNewLine]", \(\fF =
  uU - tT;\), "[IndentingNewLine]",
StyleBox[\( (* fF is the total energy functional \ * ) \),
  FontColor->RGBColor[1, 0,
0]], "[IndentingNewLine]", \(\eq1 =
  D[fF, a00];\), "[IndentingNewLine]", \(\eq2 =
  D[fF, a02];\), "[IndentingNewLine]",
RowBox[{\(eq3 = D[fF, a20];\),
  "[IndentingNewLine]"}, \(\[IndentingNewLine]", \(\eqs =
  LinearEquationsToMatrices[{\eq1 \[Equal] 0, eq2 \[Equal] 0,
    eq3 \[Equal] 0}, {a00, a02,
    a20};\), "[IndentingNewLine]", \(\deteqs =
  eqs[\{1\}];\), "[IndentingNewLine]", \(\Print[
theequation]), "[IndentingNewLine]", \(\polinomialeq =
  Det[deteqs] \ (*
    the determinant of the equations \ * ) ;\), "[IndentingNewLine]", \
\(\Print[rootsoftheequation]), "[IndentingNewLine]", \(\sol =
  Solve[polinomialeq \[Equal]
    0, \[\Lambda];\), "[IndentingNewLine]", \(\Print[
r]), "[IndentingNewLine]", \(\trfrsolution =
  N[sol^0.5*\@2*
    b^2]), "[IndentingNewLine]", \(\TimeUsed[]), \
  "[IndentingNewLine]",
  RowBox[{"bitti", "[IndentingNewLine]"}, "[IndentingNewLine]", \(\r =
  7.0), "[IndentingNewLine]",
  RowBox[{\(b = a/r\),
    "[IndentingNewLine]"}, \(\[IndentingNewLine]", \(\d =
    1;\), "[IndentingNewLine]", \(\w = \((x^\(2\ n)/a^\(2\ n) + \
y^\(2\ n)/b^\(2\ n) - 1)\)^\w1*\((a00 + a02*y^\w2/b^\w2 +
    a20*x^\w2/a^\w2)\), "[IndentingNewLine]",
  RowBox[{\(intbound = b*\@(1 - \((x/a)^\(2\ n)\))\),
    "[IndentingNewLine]"}, \(\[IndentingNewLine]", \(\uUt =
  d^\w2*Integrate[\((D[w, {x, 2}] + D[w, {y, 2}])^\w2 +
    2*\((1 - \[Nu])\)*\((D[D[w, y], x])^\w2 -
    D[w, {x, 2}]*D[w, {y, 2}])\), {y, \(-intbound),
    intbound};\), "[IndentingNewLine]", \(\uU =
  Integrate[uUt, {x, \(-1), 1};\), "[IndentingNewLine]",
  RowBox[{\
  StyleBox[\( (* uU is the strain energy due to bending \ * ) \),
    FontColor->RGBColor[1, 0, 0]], "[IndentingNewLine]",
  StyleBox[
    RowBox[{"*", " "},
    RowBox[{"d", "="},
    RowBox[{\
      FractionBox[
        SuperscriptBox[

```

```

StyleBox["Eh",
  FontColor->RGBColor[1, 0, 0],
  "3"], \[12 \((1 - \[Nu]^\[2])\)\)], " ", "is", " ", "the",
  " ", "flexural", " ", "rigidity", " ", "of", " ", "the", " ",
  "plate"}]], " ", "*""}],
FontColor->RGBColor[1, 0,
0]]], "\[IndentingNewLine]", \[tTt = \[Lambda]*
Integrate[
  w^\[2], {y, \(-intbound\),
  intbound};\)], "\[IndentingNewLine]", \[tT =
  Integrate[tTt, {x, \(-1\), 1};\)], "\[IndentingNewLine]",
StyleBox[\(( * \[Lambda] = 1/2*\[Rho]*h*\[Omega]^\[2] \ * ) \)],
FontColor->RGBColor[1, 0, 0]], "\[IndentingNewLine]",
StyleBox[\(( * \[tT] is the kinetic energy * ) \)],
FontColor->RGBColor[1, 0, 0]], "\[IndentingNewLine]", \[Print[
thisisfF]], "\[IndentingNewLine]", \[fF =
  uU - tT;\)], "\[IndentingNewLine]",
StyleBox[\(( * \[fF] is the total energy functional * ) \)],
FontColor->RGBColor[1, 0,
0]], "\[IndentingNewLine]", \[eq1 =
  D[fF, a00];\)], "\[IndentingNewLine]", \[eq2 =
  D[fF, a02];\)], "\[IndentingNewLine]",
RowBox[{\[eq3 = D[fF, a20];\)],
"\[IndentingNewLine]"}, "\[IndentingNewLine]", \[eqs =
  LinearEquationsToMatrices[{\[eq1] \[Equal] 0, \[eq2] \[Equal] 0,
  \[eq3] \[Equal] 0}, {a00, a02,
  a20};\)], "\[IndentingNewLine]", \[deteqs =
  eqs[\[1]]; \)], "\[IndentingNewLine]", \[Print[
theequation]], "\[IndentingNewLine]", \[polinomialeq =
  Det[deteqs] \ ( * \
  the determinant of the equations * ) ;\)], "\[IndentingNewLine]", \
\[Print[rootsoftheequation]], "\[IndentingNewLine]", \[sol =
  Solve[polinomialeq \[Equal]
  0, \[Lambda];\)], "\[IndentingNewLine]", \[Print[
r]], "\[IndentingNewLine]", \[trfrsolution =
  N[sol^\[0.5*\[2*
  b^\[2]), "\[IndentingNewLine]", \[TimeUsed[ ]], \
"\[IndentingNewLine]",
RowBox[{"bitti", "\[IndentingNewLine]"}], "\[IndentingNewLine]", \[r =
  8.0\)], "\[IndentingNewLine]",
RowBox[{\(b = a\sqrt{r}\),
"\[IndentingNewLine]"}], "\[IndentingNewLine]", \[d =
  1;\)], "\[IndentingNewLine]", \[w = \((x^\[2] \[2] n)/a^\[2] \[2] n) + \
y^\[2] \[2] n)/b^\[2] \[2] n) - 1)\)^\[1] * \((a00 + a02*y^\[2] \[2] n +
  a20*x^\[2] \[2] n)\)], "\[IndentingNewLine]",
RowBox[{\(intbound = b*\[2] \[2] n) \((1 - \((x/a))^\[2] \[2] n)\)\)],
"\[IndentingNewLine]"}, "\[IndentingNewLine]", \[uUt =
  d/2*Integrate[\((D[w, {x, 2}] + D[w, {y, 2}])\)\^\[2] +
  2*\((1 - \[Nu])\)*\((D[D[w, y], x])\)\^\[2] -
  D[w, {x, 2}]*D[w, {y, 2}])\)], {y, \(-intbound\),
  intbound};\)], "\[IndentingNewLine]", \[uU =
  Integrate[uUt, {x, \(-1\), 1};\)], "\[IndentingNewLine]",
RowBox[{\
StyleBox[\(( * uU is the strain energy due to bending * ) \)],
FontColor->RGBColor[1, 0, 0]], "\[IndentingNewLine]",

```

```

StyleBox[
  RowBox[{"(*", " ",
    RowBox[{"d", "=",
      RowBox[
        FractionBox[
          SuperscriptBox[
            StyleBox["Eh",
              FontColor->RGBColor[1, 0, 0]],
            "3"], \((1 - \sqrt{1 - \nu^2})\)), " ", "is", " ", "the",
            " ", "flexural", " ", "rigidity", " ", "of", " ", "the", " ",
            "plate"}]], " ", "*)"}],
    FontColor->RGBColor[1, 0,
0]]], "\[IndentingNewLine]", \((tT = \sqrt{\lambda} *
  Integrate[
    w^2, {y, \(-intbound\),
      intbound};\), "\[IndentingNewLine]", \((tT =
    Integrate[tT, {x, \(-1\), 1};\), "\[IndentingNewLine]",
StyleBox[\(( * \sqrt{\lambda} = 1/2 * \rho * h * \omega^2 \backslash * ) \),
  FontColor->RGBColor[1, 0, 0]], "\[IndentingNewLine]",
StyleBox[\(( * \backslash tT \backslash is \ the \ kinetic \ energy \ * ) \),
  FontColor->RGBColor[1, 0, 0]], "\[IndentingNewLine]", \((Print[
thisisfF]), "\[IndentingNewLine]", \((fF =
  uU - tT;\), "\[IndentingNewLine]",
StyleBox[\(( * \ fF \ is \ the \ total \ energy \ functional \ * ) \),
  FontColor->RGBColor[1, 0,
0]], "\[IndentingNewLine]", \((eq1 =
  D[fF, a00];\), "\[IndentingNewLine]", \((eq2 =
  D[fF, a02];\), "\[IndentingNewLine]",
RowBox[{\(eq3 = D[fF, a20];\),
"\[IndentingNewLine]"}, "\[IndentingNewLine]", \((eqs =
  LinearEquationsToMatrices[ {eq1 \[Equal] 0, eq2 \[Equal] 0,
    eq3 \[Equal] 0}, {a00, a02,
    a20};\), "\[IndentingNewLine]", \((deteqs =
    eqs[1];\), "\[IndentingNewLine]", \((Print[
theequation]), "\[IndentingNewLine]", \((polinomialeq =
  Det[deteqs] \backslash ( * \
    the \ determinant \ of \ the \ equations \ * ) ;\), "\[IndentingNewLine]", \
\((Print[rootsoftheequation]), "\[IndentingNewLine]", \((sol =
  Solve[polinomialeq \[Equal]
    0, \sqrt{\lambda}];\), "\[IndentingNewLine]", \((Print[
r]), "\[IndentingNewLine]", \((trfrsolution =
  N[sol^0.5 * @2 *
    b^2]), "\[IndentingNewLine]", \((TimeUsed[ ]), \
"\[IndentingNewLine]",
  RowBox[{"bitti", "\[IndentingNewLine]"}, "\[IndentingNewLine]", \((r =
  9.0), "\[IndentingNewLine]",
  RowBox[{\(b = a/r\),
    "\[IndentingNewLine]"}, "\[IndentingNewLine]", \((d =
    1;\), "\[IndentingNewLine]", \((w = \((x^{\(2 n\)} / a^{\(2 n\)} + \
y^{\(2 n\)} / b^{\(2 n\)} - 1)\)^1 * (a00 + a02 * y^2 / b^2 +
    a20 * x^2 / a^2)), "\[IndentingNewLine]",
  RowBox[{\(intbound = b * @ \sqrt{1 - ((x/a))^{\(2 n\)}}\),
    "\[IndentingNewLine]"}, "\[IndentingNewLine]", \((uU =
    d \sqrt{2} * Integrate[\((D[w, {x, 2}] + D[w, {y, 2}])\)^2 +
    2 * (1 - \nu) \backslash \((D[D[w, y], x])\)^2 -

```

```

D[w, {x, 2}]*D[w, {y, 2}]]))\), {y, \(-intbound\),
intbound};\), "\[IndentingNewLine]", \(\uU =
Integrate[uUt, {x, \(-1\), 1}];\), "\[IndentingNewLine]",
RowBox[{
StyleBox[\( (* \uU is the strain energy due to bending *) \),
FontColor->RGBColor[1, 0, 0]], "\[IndentingNewLine]",
StyleBox[
RowBox[{"(*", " ",
RowBox[{"d", "=",
RowBox[{
FractionBox[
SuperscriptBox[
StyleBox["Eh",
FontColor->RGBColor[1, 0, 0]],
"3"], \((1 - \[Nu]^2)\)], " ", "is", " ", "the",
" ", "flexural", " ", "rigidity", " ", "of", " ", "the", " ",
"plate"}]], " ", "*)"}],
FontColor->RGBColor[1, 0,
0]]}], "\[IndentingNewLine]", \(\tT = \[Lambda]*
Integrate[
w^2, {y, \(-intbound\),
intbound};\), "\[IndentingNewLine]", \(\tT =
Integrate[tTt, {x, \(-1\), 1}];\), "\[IndentingNewLine]",
StyleBox[\( (* \[Lambda] = 1/2*\[Rho]*h*\[Omega]^2\ *) \),
FontColor->RGBColor[1, 0, 0]], "\[IndentingNewLine]",
StyleBox[\( (* \tT is the kinetic energy *) \),
FontColor->RGBColor[1, 0, 0]], "\[IndentingNewLine]", \(\Print[
thisisF]), "\[IndentingNewLine]", \(\fF =
uU - tT;\), "\[IndentingNewLine]",
StyleBox[\( (* fF is the total energy functional *) \),
FontColor->RGBColor[1, 0,
0]], "\[IndentingNewLine]", \(\eq1 =
D[fF, a00];\), "\[IndentingNewLine]", \(\eq2 =
D[fF, a02];\), "\[IndentingNewLine]",
RowBox[{\(eq3 = D[fF, a20];\),
"\[IndentingNewLine]"}], "\[IndentingNewLine]", \(\eqs =
LinearEquationsToMatrices[{eq1 \[Equal] 0, eq2 \[Equal] 0,
eq3 \[Equal] 0}, {a00, a02,
a20}];\), "\[IndentingNewLine]", \(\deteqs =
eqs[\[1]]; \), "\[IndentingNewLine]", \(\Print[
theequation]), "\[IndentingNewLine]", \(\polinomialeq =
Det[deteqs] \ (*\
the determinant of the equations *) ;\), "\[IndentingNewLine]", \
\(\Print[rootsoftheequation]), "\[IndentingNewLine]", \(\sol =
Solve[polinomialeq \[Equal]
0, \[Lambda];\), "\[IndentingNewLine]", \(\Print[
r]), "\[IndentingNewLine]", \(\trfrsolution =
N[sol^0.5*@\2*
b^2]), "\[IndentingNewLine]", \(\TimeUsed[]), \
"\[IndentingNewLine]",
RowBox[{"bitti", "\[IndentingNewLine]"}], "\[IndentingNewLine]", \(\r =
10.0\), "\[IndentingNewLine]",
RowBox[{\(b = a\sqrt{r}),
"\[IndentingNewLine]"}], "\[IndentingNewLine]", \(\d =
1;\), "\[IndentingNewLine]", \(\w = \((x^\(2\ n)/a^\(2\ n) + \

```

```

y^(2\ n)/b^(2\ n) - 1))^(1*(a00 + a02*y^2/b^2 +
a20*x^2/a^2))), "[IndentingNewLine]",
RowBox[{(intbound = b*@((1 - ((x/a))^(2\ n))))},
"[IndentingNewLine"]}], "[IndentingNewLine]", (uU =
d\sqrt{2}*Integrate[(D[w, {x, 2}] + D[w, {y, 2}])^2 +
2*((1 - \[Nu])*(D[D[w, y], x])^2 -
D[w, {x, 2}]*D[w, {y, 2}])], {y, (-intbound),
intbound}], "[IndentingNewLine]", (uU =
Integrate[uU, {x, (-1), 1}];), "[IndentingNewLine]",
RowBox[{
StyleBox[( (* uU is the strain energy due to bending *) ),
FontColor->RGBColor[1, 0, 0]], "[IndentingNewLine]",
StyleBox[
RowBox[{"(*", " ",
RowBox[{"d", "=",
RowBox[{
FractionBox[
SuperscriptBox[
StyleBox["Eh",
FontColor->RGBColor[1, 0, 0]],
"3"], (12 ((1 - \[Nu]^2)))]}, " ", "is", " ", "the",
" ", "flexural", " ", "rigidity", " ", "of", " ", "the", " ",
"plate"}]], " ", "*)"],
FontColor->RGBColor[1, 0,
0]]}], "[IndentingNewLine]", (tT = \[Lambda]*
Integrate[
w^2, {y, (-intbound),
intbound}];), "[IndentingNewLine]", (tT =
Integrate[tT, {x, (-1), 1}];), "[IndentingNewLine]",
StyleBox[( (* \[Lambda] = 1/2*\[Rho]*h*\[Omega]^2\ *) ),
FontColor->RGBColor[1, 0, 0]], "[IndentingNewLine]",
StyleBox[( (* tT is the kinetic energy *) ),
FontColor->RGBColor[1, 0, 0]], "[IndentingNewLine]", (Print[
thisisFF]), "[IndentingNewLine]", (fF =
uU - tT;), "[IndentingNewLine]",
StyleBox[( (* fF is the total energy functional *) ),
FontColor->RGBColor[1, 0,
0]], "[IndentingNewLine]", (eq1 =
D[fF, a00];), "[IndentingNewLine]", (eq2 =
D[fF, a02];), "[IndentingNewLine]",
RowBox[{(eq3 = D[fF, a20];),
"[IndentingNewLine"]}], "[IndentingNewLine]", (eqs =
LinearEquationsToMatrices[{eq1 [Equal] 0, eq2 [Equal] 0,
eq3 [Equal] 0}, {a00, a02,
a20}];), "[IndentingNewLine]", (deteqs =
eqs[[1]]);), "[IndentingNewLine]", (Print[
theequation]), "[IndentingNewLine]", (polinomial =
Det[deteqs] (*
the determinant of the equations *) );), "[IndentingNewLine]", \
(Print[rootsoftheequation]), "[IndentingNewLine]", (sol =
Solve[polinomial [Equal]
0, \[Lambda]]);), "[IndentingNewLine]", (Print[
r]), "[IndentingNewLine]", (trfrsolution =
N[sol^0.5*@2*
b^2]), "[IndentingNewLine]", (TimeUsed[ ]), \

```

```

"\[IndentingNewLine]",
  RowBox[{"bitti", "\[IndentingNewLine]"}, "\[IndentingNewLine]", \(\(r =
    15.0\), "\[IndentingNewLine]",
  RowBox[{\(b = a\sqrt{r}\),
    "\[IndentingNewLine]"}, "\[IndentingNewLine]", \(\(d =
    1;\), "\[IndentingNewLine]", \(\(w = \((x\^{(2\ n)}/a\^{(2\ n)} + \
y\^{(2\ n)}/b\^{(2\ n)} - 1)\)^{1*}((a00 + a02*y\^{2}/b\^{2} +
    a20*x\^{2}/a\^{2}))\), "\[IndentingNewLine]",
  RowBox[{\(intbound = b*\@{(1 - \((x/a)\)^{(2\ n))}\),
    "\[IndentingNewLine]"}, "\[IndentingNewLine]", \(\(uU =
    d\sqrt{2}*Integrate[\((D[w, {x, 2}] + D[w, {y, 2}])\)^{2} +
    2*\((1 - \[Nu])\)*\((D[D[w, y], x])\)^{2} -
    D[w, {x, 2}]*D[w, {y, 2}])\), {y, \(-intbound\),
    intbound}\), "\[IndentingNewLine]", \(\(uU =
    Integrate[uU, {x, \(-1\), 1}\];\), "\[IndentingNewLine]",
  RowBox[{\
  StyleBox[\( (* uU is the strain energy due to bending *) \),
    FontColor->RGBColor[1, 0, 0]], "\[IndentingNewLine]",
  StyleBox[
  RowBox[{"(*", " ",
    RowBox[{"d", "="},
    RowBox[{\
      FractionBox[
        SuperscriptBox[
          StyleBox["Eh",
            FontColor->RGBColor[1, 0, 0]],
          "3"], \((1 - \[Nu]\^{2})\)], " ", "is", " ", "the",
          " ", "flexural", " ", "rigidity", " ", "of", " ", "the", " ",
          "plate"}]], " ", "*)"}],
    FontColor->RGBColor[1, 0,
    0]]}], "\[IndentingNewLine]", \(\(tT = \[Lambda]*
    Integrate[
      w\^{2}, {y, \(-intbound\),
        intbound}\];\), "\[IndentingNewLine]", \(\(tT =
        Integrate[tT, {x, \(-1\), 1}\];\), "\[IndentingNewLine]",
  StyleBox[\( (* \[Lambda] = 1\sqrt{2}*\[Rho]*h*\[Omega]\^{2} \ *) \),
    FontColor->RGBColor[1, 0, 0]], "\[IndentingNewLine]",
  StyleBox[\( (* tT is the kinetic energy *) \),
    FontColor->RGBColor[1, 0, 0]], "\[IndentingNewLine]", \(\(Print[
    thisisF]\), "\[IndentingNewLine]", \(\(fF =
    uU - tT;\), "\[IndentingNewLine]",
  StyleBox[\( (* fF is the total energy functional *) \),
    FontColor->RGBColor[1, 0,
    0]], "\[IndentingNewLine]", \(\(eq1 =
    D[fF, a00];\), "\[IndentingNewLine]", \(\(eq2 =
    D[fF, a02];\), "\[IndentingNewLine]",
  RowBox[{\(eq3 = D[fF, a20];\),
    "\[IndentingNewLine]"}, "\[IndentingNewLine]", \(\(eqs =
    LinearEquationsToMatrices[{\(eq1 \[Equal] 0, eq2 \[Equal] 0,
    eq3 \[Equal] 0\}, {a00, a02,
    a20}\];\), "\[IndentingNewLine]", \(\(deteqs =
    eqs[\{1\}];\), "\[IndentingNewLine]", \(\(Print[
    theequation]\), "\[IndentingNewLine]", \(\(polinomialeq =
    Det[deteqs] \ (*
    the determinant of the equations *) \), "\[IndentingNewLine]", \

```

```

(Print[rootsoftheequation]), "[IndentingNewLine]", (sol =
  Solve[polinomialeq \[Equal]
    0, \[Lambda]];), "[IndentingNewLine]", (Print[
r]), "[IndentingNewLine]", (trfrsolution =
N[sol^0.5*\@2*
  b^2]), "[IndentingNewLine]", (TimeUsed[]), \
"[IndentingNewLine]",
RowBox[{"bitti", "[IndentingNewLine]"}, "[IndentingNewLine]", (r =
20.0), "[IndentingNewLine]",
RowBox[{(b = a/r),
  "[IndentingNewLine]"}, "[IndentingNewLine]", (d =
1;), "[IndentingNewLine]", (w = ((x^(2 n))/a^(2 n)) +
y^(2 n)/b^(2 n) - 1))^1*((a00 + a02*y^2/b^2 +
a20*x^2/a^2)), "[IndentingNewLine]",
RowBox[{(intbound = b*\@(1 - ((x/a))^(2 n))),
  "[IndentingNewLine]"}, "[IndentingNewLine]", (uUt =
d^2*Integrate[(((D[w, {x, 2}] + D[w, {y, 2}]))^2 +
2*((1 - \[Nu]))*((D[D[w, y], x]))^2 -
D[w, {x, 2}]*D[w, {y, 2}]))], {y, (-intbound),
intbound}), "[IndentingNewLine]", (uU =
Integrate[uUt, {x, (-1), 1}];), "[IndentingNewLine]",
RowBox[{
StyleBox[( (* uU is the strain energy due to bending *) ),
  FontColor->RGBColor[1, 0, 0]], "[IndentingNewLine]",
StyleBox[
RowBox[{"(*", " ",
  RowBox[{"d", "=",
  RowBox[{
FractionBox[
SuperscriptBox[
StyleBox["Eh",
  FontColor->RGBColor[1, 0, 0]],
"3"], (12 ((1 - \[Nu]^2))), " ", "is", " ", "the",
" ", "flexural", " ", "rigidity", " ", "of", " ", "the", " ",
"plate"}]}], " ", "*)"}],
FontColor->RGBColor[1, 0,
0]]}, "[IndentingNewLine]", (tTt = \[Lambda]*
Integrate[
w^2, {y, (-intbound),
intbound}];), "[IndentingNewLine]", (tT =
Integrate[tTt, {x, (-1), 1}];), "[IndentingNewLine]",
StyleBox[( (* \[Lambda] = 1/2*\[Rho]*h*\[Omega]^2 \ *) ),
  FontColor->RGBColor[1, 0, 0]], "[IndentingNewLine]",
StyleBox[( (* tT is the kinetic energy *) ),
  FontColor->RGBColor[1, 0, 0]], "[IndentingNewLine]", (Print[
thisisfF]), "[IndentingNewLine]", (fF =
uU - tT;), "[IndentingNewLine]",
StyleBox[( (* fF is the total energy functional *) ),
  FontColor->RGBColor[1, 0,
0]], "[IndentingNewLine]", (eq1 =
D[fF, a00];), "[IndentingNewLine]", (eq2 =
D[fF, a02];), "[IndentingNewLine]",
RowBox[{(eq3 = D[fF, a20];),
  "[IndentingNewLine]"}, "[IndentingNewLine]", (eqs =
LinearEquationsToMatrices[{eq1 \[Equal] 0, eq2 \[Equal] 0,

```

```

eq3 \[Equal] 0}, {a00, a02,
a20};\), "\[IndentingNewLine]", \(\deteqs =
eqs[\(1\)];\), "\[IndentingNewLine]", \(\Print[
theequation]\), "\[IndentingNewLine]", \(\polinomialeq =
Det[\deteqs]\ (*\
the\ determinant\ of\ the\ equations\ *) ;\), "\[IndentingNewLine]", \
\(\Print[rootsoftheequation]\), "\[IndentingNewLine]", \(\sol =
Solve[\polinomialeq \[Equal]
0, \[Lambda]];\), "\[IndentingNewLine]", \(\Print[
r]\), "\[IndentingNewLine]", \(\trfrsolution =
N[sol^0.5*\@2*
b^2]), "\[IndentingNewLine]", \(\TimeUsed[[]], \
"\[IndentingNewLine]", "bitti"}], "Input"
},
FrontEndVersion->"5.2 for Microsoft Windows",
ScreenRectangle->{{0, 1280}, {0, 877}},
WindowSize->{1018, 800},
WindowMargins->{{92, Automatic}, {Automatic, 0}}
]

(*****
Cached data follows. If you edit this Notebook file directly, not
using Mathematica, you must remove the line containing CacheID at
the top of the file. The cache data will then be recreated when
you save this file from within Mathematica.
*****)

(*CellTagsOutline
CellTagsIndex->{}
*)

(*CellTagsIndex
CellTagsIndex->{}
*)

(*NotebookFileOutline
Notebook[{
Cell[1754, 51, 28469, 559, 6738, "Input"]
}
]
*)
(*****
End of Mathematica Notebook file.
*****)

```

REFERENCES

- 1- Wang, C.M., L. Wang and K.M. Liew, 1994, "Vibration and buckling of super elliptical plates", *Journal of Sound and Vibration*, Vol. 171, pp. 301-314.
- 2- Altekin, M., 2005, *Static and Dynamic Analysis of Super-Elliptical Plates*, Ph.D. Thesis, Boğaziçi University.
- 3- Mohr, G.A., 1999, "Polynomial solutions for thin plates", *International Journal of Mechanical Sciences*, Vol. 42, pp. 1197-1204.
- 4- Zenkour, A.M., 2005, "A comprehensive analysis of functionally graded sandwich plates: Part 1-Deflection and stresses", *International Journal of Solids and Structures*, Vol. 42, pp. 5224-5242.
- 5- Muhammad, T. and A.V. Singh, 2004, "A p-type solution for the bending of rectangular, circular, elliptic and skew plates", *International Journal of Solids and Structures*, Vol. 41, pp. 3977-3997.
- 6- Korol, Y.Z., 2001, "The solution of boundary-value problems of the longitudinal-transverse bending of orthotropic circular plates on a linearly elastic base" *Journal of Applied Mathematics and Mechanics*, Vol. 65(6), pp. 963-975.
- 7- Shames, I.H. and C.L. Dym, 1991, *Energy and Finite Element Methods in Structural Mechanics*, Hemisphere, Washington, DC.
- 8- Wang, C.M., J.N. Reddy and K.H. Lee, 2000, *Shear Deformable Beams and Plates: Relationships with Classical Solutions*, Elsevier Science Ltd., Amsterdam.

- 9- Szillard, R., 1974, *Theory and Analysis of Plates: Classical and Numerical Methods*, Prentice-Hall, New Jersey.
- 10- Jeager, L.G., 1969, *Elementary Theory of Elastic Plates*, Pergamon Press Ltd., London.
- 11- Timoshenko S. and S. Woinowsky-Krieger, 1959, *Theory of Plates and Shells*, New York, McGraw-Hill.
- 12- Leissa, A.W., 1969, *Vibration of Plates - NASA SP-160*, US Government Printing Office, Washington, DC.
- 13- Chakraverty, S., R.B. Bhat and I. Stiharu, 2001, "Free vibration of annular elliptic plates using boundary characteristic orthogonal polynomials as shape functions in the Rayleigh-Ritz method", *Journal of Sound and Vibration*, Vol. 241(3), pp. 524-539.
- 14- Chen, J.T., I.L. Chen, K.H. Chen, Y.T. Lee and Y.T. Yeh, 2004, "A Meshless method for free vibration analysis of circular and rectangular clamped plates using radial basis function", *Engineering Analysis with Boundary Elements*, Vol. 28, pp. 534-545.
- 15- Mukherjee, M., 2001, "Forced vertical vibrations of an elastic elliptic plate on an elastic half space- a direct approach using orthogonal polynomials", *International Journal of Solids and Structures*, Vol. 38, pp. 389-399.
- 16- Bayer, I., U. Güven and G. Altay, 2002, "A parametric study on vibrating clamped elliptical plates with variable thickness", *Journal of Sound and Vibration*, Vol. 254(1), pp. 179-188.
- 17- Chen, C.C., C.W. Lim, S. Kitipornchai and K.M. Liew, 1999, "Vibration of symmetrically laminated thick super elliptical plates", *Journal of Sound and Vibration*, Vol. 220(4), pp. 659-682.

- 18- Leissa, A.W., 1967, "Vibration of a simply-supported elliptical plate", *Journal of Sound and Vibration*, Vol. 6(1), pp. 145-148.
- 19- Sato, K., 1972, "Free flexural vibrations of an elliptical plate with simply supported edge", *Journal of the Acoustical Society of America*, Vol.52, pp.919-922.
- 20- Narita, Y., 1985, "Natural frequencies of free, orthotropic elliptical plates", *Journal of Sound and Vibration*, Vol. 100(1), pp. 83-89.
- 21- Narita, Y., 1986, "Free vibration analysis of orthotropic elliptical plates resting on arbitrarily distributed point supports", *Journal of Sound and Vibration*, Vol. 108(1), pp. 1-10.
- 22- Zhou, D., S.H. Lo, and F.T.K. Au, 2004, "3-D vibration analysis of generalized super elliptical plates using Chebyshev-Ritz method", *International Journal of Solids and Structures*, Vol. 41, pp. 4697-4712.
- 23- Tezcan, S.S., 1967, "Nonlinear analysis of thin plates by framework method", *AIAA Journal*, Vol. 5, pp. 1890-1967.
- 24- Prakash, T. and M. Ganapathi, 2006, "Asymmetric flexural vibration and thermoelastic stability of FGM circular plates using finite element method", *Composites: Part B*, Vol. 37, pp. 642-649.
- 25- Koizumi, M., 1997, "FGM activities in Japan", *Composites Part B*, Vol. 28, pp. 1-4.
- 26- Amada, S., Y. Ichikawa, T. Munekata, Y. Nagase and H. Shimizu, 1997, "Fiber texture and mechanical graded structure of bamboo", *Composites Part B*, Vol. 28, pp. 13-20.
- 27- Ferreira, A.J.M., R.C. Batra, C.M.C. Roque, L.F. Qian, and R.M.N. Jorge, 2006, "Natural frequencies of functionally graded plates by a meshless method", *Composite Structures*, Vol. 75, pp. 593-600.

- 28- Suresh, S., 1997, "Modeling and design of multi-layered and graded materials", *Progress in Materials Science*, Vol. 42, pp. 243-251.
- 29- Chi, S.H. and Y.L. Chung, 2006, "Mechanical behavior of functionally graded material plates under transverse load-Part I: Analysis", *International Journal of Solids and Structures*, Vol. 43, pp. 3657-3674.
- 30- Chi, S.H. and Y.L. Chung, 2006, "Mechanical behavior of functionally graded material plates under transverse load-Part II: Numerical results", *International Journal of Solids and Structures*, Vol. 43, pp. 3675-3691.
- 31- Cheng, Z.Q. and R.C. Batra, 2000, "Exact correspondence between eigenvalues of membranes and functionally graded simply supported polygonal plates", *Journal of Sound and Vibration*, Vol. 229(4), pp. 879-895.
- 32- Croce, L.D. and P. Venini, 2004, "Finite elements for functionally graded Reissner-Mindlin plates", *Computer Methods in Applied Mechanics and Engineering*, Vol. 193, pp. 705-725.
- 33- Ruys, A.J., E.B. Popov, D. Sun, J.J. Russell and C.C.J. Murray, 2001, "Functionally graded electrical/thermal ceramic systems", *Journal of the European Ceramic Society*, Vol. 21, pp. 2025-2029.
- 34- Liew, K.M., X.Q. He, T.Y. Ng and S. Sivashanker, 2001, "Active control of FGM plates subjected to a temperature gradient: Modeling via finite element method based on FSDT", *International Journal for Numerical Methods in Engineering*, Vol. 52, pp. 1253-1271.
- 35- He, X.Q., T.Y. Ng, S. Sivashanker and K.M. Liew, 2001, "Active control of FGM plates with integrated piezoelectric sensors and actuators", *International Journal of Solids and Structures*, Vol. 38, pp. 1641-1655.

- 36- Vel, S.S. and R.C. Batra, 2004, "Three-dimensional exact solution for the vibration of functionally graded rectangular plates", *Journal of Sound and Vibration*, Vol. 272, pp. 703-730.
- 37- Ng, T.Y., K.Y. Lam and K.M. Liew, 2000, "Effects of FGM materials on the parametric resonance of plate structures", *Computer Methods in Applied Mechanics and Engineering*, Vol. 190, pp. 953-962.
- 38- C.A.J. Fletcher, 1984, *Computational Galerkin Methods*, Springer-Verlag, New York.
- 39- Liu, L., L.P. Chua and D.N. Ghista, 2006, "Element free Galerkin Method for static and dynamic analysis of spatial shell structures", *Journal of Sound and Vibration*, Vol. 295, pp. 388-406.
- 40- Dai, K.Y., G.R. Liu, X. Han and K.M. Lim, 2005, "Thermomechanical analysis of functionally graded material (FGM) plates using element-free Galerkin method", *Computers and Structures*, Vol. 83, pp. 1487-1502.
- 41- Crandall, S.H., 1956, *Engineering Analysis, A Survey of Numerical Procedures*, McGraw-Hill, New York.
- 42- Strang, G., *Engineering Analysis, Introduction to Applied Mathematics*, Wellesley-Cambridge, Massachusetts.
- 43- Kaliakin, V.N., 2002, *Introduction to Approximate Solution Techniques, Numerical Modeling, and Finite Element Methods*, Marcel Dekker, New York.
- 44- Shisha, O., 1968, "Trends in approximation theory", *Applied Mechanics Reviews*, Vol. 21(4), pp. 337-341.

45- Delale, F. and F. Erdogan, 1983, "The crack problem for a non-homogeneous plane", *ASME Journal of Applied Mechanics*, Vol. 50, pp. 609-614.